

**Study the Effect of Topology on the Performance of an Advanced Metering
Infrastructure Network**

by

Thobekile Joyce Ngcobo

Submitted in fulfilment of the academic requirements of

Master of Science

in Electrical Engineering

College of Agriculture, Engineering and Science

University of KwaZulu-Natal

Durban

South Africa

December 2021

PREFACE

The research contained in this dissertation was completed by the candidate while based in the Discipline of Electrical Engineering, School of Engineering of the College of Agriculture, Engineering and Science, University of KwaZulu-Natal, Howard College, South Africa. The research was financially supported by Eskom.

The contents of this work have not been submitted in any form to another university and, except where the work of others is acknowledged in the text, the results reported are due to investigations by the candidate.

Signed: Dr. Farzad Ghayoor

Date: December 2021

DECLARATION 1: PLAGIARISM

I, Thobekile Joyce Ngcobo, declare that:

(i) the research reported in this dissertation, except where otherwise indicated or acknowledged, is my original work;

(ii) this dissertation has not been submitted in full or in part for any degree or examination to any other university;

(iii) this dissertation does not contain other persons' data, pictures, graphs or other information, unless specifically acknowledged as being sourced from other persons;

(iv) this dissertation does not contain other persons' writing, unless specifically acknowledged as being sourced from other researchers. Where other written sources have been quoted, then:

a) their words have been re-written but the general information attributed to them has been referenced;

b) where their exact words have been used, their writing has been placed inside quotation marks, and referenced;

(v) where I have used material for which publications followed, I have indicated in detail my role in the work;

(vi) this dissertation is primarily a collection of material, prepared by myself, published as journal articles or presented as a poster and oral presentations at conferences. In some cases, additional material has been included;

(vii) this dissertation does not contain text, graphics or tables copied and pasted from the Internet, unless specifically acknowledged, and the source being detailed in the dissertation and in the References sections.

Signed: Thobekile Joyce Ngcobo

Date: December 2021

DECLARATION 2: PUBLICATIONS

DETAILS OF CONTRIBUTION TO PUBLICATIONS that form part and/or include research presented in this dissertation:

T.J. Ngcobo, F. Ghayoor. *Study the Topology Effect on a G3-PLC based AMI Network*. 2019 Southern African Universities Power Engineering Conference/Robotics and Mechatronics/Pattern Recognition Association of South Africa (SAUPEC/RobMech/PRASA), Bloemfontein, Jan. 2019

The paper was authored by T.J. Ngcobo and co-authored by F. Ghayoor.

Signed: T.J. Ngcobo

Date: December 2021

ABSTRACT

A smart grid operates based on the integration of various renewable energy sources, distributed generators and storage units in order to deliver an uninterrupted energy supply to consumers. Such a complex grid requires a network of intelligent sensors and an effective communication infrastructure to provide bi-directional flows of information between different grid entities for monitoring and control purposes. A crucial part of the smart grid communication network is the advanced metering infrastructure connecting a utility company to end-users to support telemetry and remote-control applications. Although different technologies and standards for smart metering systems exist, the G3-PLC standard, which uses the power-line communication (PLC) technology, is the accepted standard in South Africa for connecting smart meters to data concentrators. Studying the topology of an AMI network can help improve the network's Quality-of-Service to support more advanced applications. The analytical analysis is usually considered a viable method for studying the topological effect on the performance of PLC-based AMI networks, as physically altering such networks can become very costly. Therefore, in this research, such methods have been used to investigate the effect of topology on the performance of the G3-PLC AMI network. To better understand the system, an overview of the G3-PLC standard for smart metering application has been covered. This includes covering the DLMS/COSEM protocol at the application layer and its relation to the G3-PLC. This follows by providing the mathematical model for the G3-PLC AMI network to study the effect of topology on its performance. Based on the provided method, first, the distances between data concentrators and smart meters are identified. Then the graph theory has been used to calculate the transfer function between every node in the system for obtaining the system's total capacity. It was shown that the performance of the system decreases as longer branches are added to the network.

ACKNOWLEDGMENTS

To College of agriculture, Engineering and science, UKZN, thank you so much for allowing me this opportunity to do this research in order for me to attain master's degree.

I would like to extend my many thanks to Dr. Farzad Ghayoor for his undying patience and encouragement towards me, he stood by me every step of the way, advising and guiding me. He whole heartedly believed in me finishing this dissertation. I am more fortunate to have such a supervisor who never gave up on me, or ignored my calls and emails with queries, he always responded positively all the time.

My daughters, Qophelo and Lowami, thank you so much for always believing in me, encouraging me never to stop even when I felt weary and demotivated. I had to have late nights and early mornings, much less attention and time to spend with you during my studies, but you believed that mom was going to finish this dissertation and come back to you a better person in life.

Mom, Madlala Jabulile, you showed us, your girls, that nothing is beyond our hands, along the way life gets tough, the trick is never to stop until the goals are fulfilled. Thank you, without your resilience in life I wouldn't be the person that I've grown to be today. Much love for you.

To my siblings, Tholi, Dolie, Ntokozo, Thobekile, Daisy and Boetana, you knew it was never easy on me, but you all kept reminding me that I need to bring this qualification and more to come home. I could always imagine the day when you celebrate and say "congratulations sister we knew you were going to bring it home"

My friends and colleagues, we are together because we understand the greatness of being a learned community, may we never stop supporting each other in life and beyond.

TABLE OF CONTENTS

	<u>Page</u>
PREFACE	ii
DECLARATION 1: PLAGIARISM.....	iii
ABSTRACT	v
ACKNOWLEDGMENTS.....	vi
TABLE OF CONTENTS	vii
LIST OF TABLES	ix
LIST OF FIGURES.....	x
LIST OF ACRONYMS AND ABBREVIATIONS.....	xii
Chapter 1 : INTRODUCTION	1
1.1. Introduction	1
1.2. Motivation	2
1.3. Problem Statement and Methodology	3
1.4. Aims and Objectives	4
1.5. Outline of Dissertation	4
Chapter 2 : LITERATURE REVIEW	5
2.1. Introduction	5
2.2. Smart Metering Systems	6
2.3. Communication Requirements for Potential Smart Metering Applications	8
2.3.1. General Requirements	8
2.3.2. Technical Requirements	9
2.4. Smart Metering Technologies and Standards.....	10
2.4.1. Wireless Technologies.....	10
2.4.2. Power-line Communication Technologies.....	11
2.4.3. Standards.....	12
2.5. Studies on the PLC-based AMI Networks	16
2.6. Summary	19
Chapter 3 : SMART METERING STANDARDS IN SOUTH AFRICA	20
3.1. Introduction	20
3.2. DLMS/COSEM.....	21

3.3. Transport and Network Layer	26
3.4. Data-Link Layer	26
3.5. Physical Layer	29
3.6. Summary	32
CHAPTER 4 : MODELLING AND SIMULATION	34
4.1. Introduction	34
4.2. Load Modelling	35
4.3. PLC Channel Model.....	37
4.4. Noise and Disturbances in NB-PLC.....	42
4.5. Channel Capacity	44
4.6. Topology Modelling.....	44
4.7. Calculating Channel Transfer Function	47
4.8. Summary	48
Chapter 5 : RESULTS AND DISCUSSIONS	49
5.1. Introduction	49
5.2. Sequential Topology	49
5.3. Parallel Topology	50
5.4. Random Topology.....	54
5.5. Performance Comparison.....	55
5.6. Summary	56
Chapter 6 : CONCLUSION AND RECOMMENDATION	57
6.1. Conclusion.....	57
6.2. Recommendation.....	59
REFERENCES.....	60

LIST OF TABLES

<u>Table</u>	<u>Page</u>
Table 2-1: Overview of typical data-rate and latency requirements for different SG applications.	10
Table 2-2: Comparison between using wireless and PLC technologies in the AMI.....	10
Table 2-3: Commonly used standards in the AMI's NAN.....	12
Table 2-4: An overview of the technical characteristic of the NB-PLC standards	15
Table 3-1: Value of group C for electricity energy (A=1)	23
Table 3-2: RS encoders based on modulation	30
Table 3-3: Data rate for various G3-PLC modulation and coding schemes	32

LIST OF FIGURES

<u>Figure</u>	<u>Page</u>
Figure 2.1. An AMI network and its components [27]	6
Figure 2.2. OSI layer mapping of AMI NAN standards [13].	16
Figure 3.1. OSI layer mapping for metering application in G3-PLC.....	21
Figure 3.2. Example of COSEM object models.....	23
Figure 3.3. DLMS/COSEM supported by G3-PLC protocol.....	25
Figure 3.4. The 6LoWPAN frame format for the G3-PLC.....	27
Figure 3.5. The messaging in LOAD protocol.....	27
Figure 3.6. A typical MAC layer data frame.....	28
Figure 3.7. A typical physical layer frame format	29
Figure 3.8. Block diagram of the G3-PLC transmitter at the physical layer.....	29
Figure 3.9. Convolutional encoder used in the G3-PLC	31
Figure 4.1. A typical LV distribution system.....	35
Figure 4.2. Typical load distribution for urban residential sector	36
Figure 4.3. A two-port network.....	38
Figure 4.4. Transfer functions for the cable link of different length in the CENELEC-A band	40
Figure 4.5. A simple LV distribution network.....	40
Figure 4.6. A simple two segment network	41
Figure 4.7. A simple network with parallel paths	41
Figure 4.8. The layout of a typical urban residential area and its LV distribution network	45
Figure 4.9. The model of the residential layout considered to study the topological effects... 46	

Figure 4.10. The pseudocode for generating a random topology for the AMI network	47
Figure 4.11. The pseudocode for calculating $T\mathbf{0}, \mathbf{i}$ between the DC and meter \mathbf{i}	47
Figure 5.1. The considered sequential topology	49
Figure 5.2. The tree graph for the considered sequential topology.....	50
Figure 5.3. The considered parallel topologies (a) Type 1 (b) Type 2.....	51
Figure 5.4. The tree graph for the considered parallel topologies (a) Type 1 (b) Type 2.....	52
Figure 5.5. (a) A random topology layout and (b) its graph tree	54
Figure 5.6. The average magnitude of transfer function for different topologies for CENELEC-A band	56

LIST OF ACRONYMS AND ABBREVIATIONS

AA	Application Association
ACSE	Application Control Service Element
AMI	Advanced Metering Infrastructure
AMR	Automated Meter Reading
AP	Application Process
APDU	Application Protocol Data Unit
DC	Data Concentrator
DLMS/COSEM	Device Language Message Specification/Companion Specification for Energy Metering
DLMS UA	DLMS User Association
DSM	Demand-Side Management
xDLMS_ASE	Extended DLMS application service element
GHG	GreenHouse Gas
HAN	Home-Area Network
IC	Interface Class
IEC	International Electrotechnical Commission
IP	Internet Protocol
LD	Logical Devices
LN	Logical Name
MAC	Medium Access Control
MDMS	Meter Data Management Systems
NAN	Neighbourhood-Area Network
OBIS	Object Identification System
PLC	Power-Line Communication
QoS	Quality-of-Service
RES	Renewable Energy Sources
RF	Radio Frequency
SAP	Service Access Point
SG	Smart Grid
SN	Short Name
SM	Smart Meter
TOU	Time-of-Use

UC	Utility Company
UDP	User Datagram Protocol
WAN	Wide-Area Network

Chapter 1 : INTRODUCTION

1.1. Introduction

South Africa has been facing an energy crisis since 2007, and despite many efforts that have been made to alleviate the problem, there is still no clear indication of the time of termination of this situation. The two main approaches considered to tackle the energy crisis in the long term are generating electricity from renewable sources of energy and deploying energy-efficiency mechanisms. Moreover, as around 80% of the generated electricity worldwide is produced from burning fossil fuels, employing renewable energy sources (RES) and energy-efficiency techniques would have a significant role in the reduction of greenhouse gas (GHG) emission [1].

Although distributed generation based on RES has attracted significant attention, the successful integration of such sources into the grid requires a certain level of interaction between utility companies (UCs) and producers. In opposed to a conventional grid, where the energy flow is unidirectional from power generators to end-users, a Smart Grid (SG) system supports a bi-directional flow of energy between different grid entities, enabling the integration of distributed generators into the grid [2]. As a result of this bi-directional flow of energy, end-users, which are known as prosumers in the SG context, can supply their excessive generated energy to the grid, helping the grid to overcome its energy shortages in the other parts. However, to obtain the required level of monitoring and control, in addition to this bi-directional flow of energy, a bi-directional flow of information between different grid entities is needed [3]. This bi-directional flow of information enables the SG to address many of the existing grid's challenges, including the overloading problem through supporting power management, demand control and energy-efficiency mechanisms [4]. Therefore, the bi-directional flow of energy and information can be considered the essential factors is establishing an SG system.

In the future power grid, more interactions between customers and UCs would exist, leading to many opportunities for developing new applications. Based on a market research, it is estimated that the SG market rises to \$50.65 billion by 2022. The estimation is by forecasting the market value in 2017, which was \$20.83 billion [5]. Such market growth has attracted much attention to research and development in the area of the SG. In South Africa, the efforts on rolling out the SG have been initiated by the Department of Energy, and as part of these efforts,

a base project with the focus on piloting an Advanced Metering Infrastructure (AMI) for residential and commercial sectors has been defined. Implementation of inclining block tariff, Time-of-Use (TOU) tariff and load limiting are considered to be achieved as part of this pilot project.

1.2. Motivation

Constant monitoring and control of the grid are the essential parts of the SG operation. To achieve this, having a widespread sensor network for monitoring the grid's status and an effective communication infrastructure for transferring the collected information and control signals across the grid is required. In fact, it is not far from reality to claim that the SG's success depends on the reliability of its deployed communication network [6]. The smart metering system is a major part of the SG's monitoring and communication network, and its establishment is considered as an early step in the realization of the SG [7].

A smart metering system, which is also known as the AMI, is a telemetry and control network in the SG that connects the grid's end-users to a UC's backhaul systems. The AMI employs information and communication technology for providing bi-directional communication links between smart meters (SMs) on the prosumer's side and the UC's data and control centres [8]. In an AMI network, SMs send information to the UC's data centres and receive notifications and control commands from the UC's control centres. An AMI network, based on its geographical expansion, is divided into three sub-networks. This research focuses on the part of the AMI network that covers data transmission between SMs and data concentrators (DCs).

In addition to the typical power consumption measurement, AMI is capable of supporting advanced applications, such as load management and controlling distributed generation and storage units [9-11]. To effectively support SG applications, an AMI network has to meet a specific level of interoperability, scalability, security and Quality-of-Service (QoS) depending on the considered SG application [12]. The QoS demonstrates the reliability of communication links and their performance in the sense of data-rate and latency. Similar to any other communication network, achieving a certain level of QoS requires careful considerations as it can be affected by different factors.

Different technologies and standards have been used in smart metering systems across the globe [13, 14]. The proposed standard for South Africa's AMI network has been discussed in SANS 62056-21 document [15]. According to this document, which is drafted by the South African Bureau of Standards (SABS), the Device Language Message Specification/Companion Specification for Energy Metering (DLMS/COSEM) has been considered as the data exchange protocol between SMs and the UC. The DLMS/COSEM can be implemented over wireless and power-line communication (PLC) technologies. Although the document has not suggested any technologies or standards for the lower layers of the AMI network, the G3-PLC has been widely used by ESKOM to connect SMs to DCs, and it can be considered as the de facto standard for the AMI's neighbourhood-area network (NAN) in South Africa.

1.3. Problem Statement and Methodology

In the G3-PLC based AMI network used in South Africa, SMs are located close to consumers' premises and should communicate with a DC that is installed on the secondary distribution transformer or inside a distribution cabinet. Each SM can act as a repeater for the other nearby SMs to extend the network coverage. Also, the use of stand-alone repeaters can be considered in special cases for reducing the cost. Currently, the considered applications of the AMI in South Africa are the remote recording of power consumption, implementation of TOU tariff and load limiting. Although such applications are not much sensitive to data-transmission latencies and communication outages, employing the AMI for more advanced SG applications requires further considerations. Similar to any other communication network, the topology of the network should have an effect on the overall performance of the system. Therefore, in this study, we investigate the effect of topology on the average capacity of an AMI NAN.

In order to thoroughly investigate a PLC-based AMI system, one needs to have access to the power grid infrastructure. However, studying the effects of network parameters and topology on an actual AMI network can become very expensive. Simulation tools, on the other hand, are feasible approaches that can provide an insight into the effect of topology on the performance of a PLC-based AMI network. Therefore, our study is based on theoretical and numerical analysis rather than a field test.

1.4. Aims and Objectives

The main aim of this research is to study the effect of topology on the performance of a G3-PLC AMI network. The following objectives are considered for achieving this goal:

- To study the AMI network and its components.
- To study the DLMS/COSEM and G3-PLC standard.
- To simulate a PLC-based AMI network in-line with the G3-PLC standard.
- To analyse the performance of the system based on the topology of a G3-PLC AMI network.

1.5. Outline of Dissertation

The rest of this dissertation is organised as follows:

Chapter 2 gives an overview of the AMI network. Moreover, different SG applications supported by the AMI and their communication requirements are covered. Thereafter, the technologies and standards employed in AMI networks' development are reviewed. Finally, an overview of the literature on modelling, analysing and optimizing of PLC-based AMI networks have been covered.

Chapter 3 focuses on outlining the G3-PLC standard. The specification of the standard at each layer is identified. This includes the DLMS/COSEM at the application layer and the support it gets from the G3-PLC to perform smart metering applications.

Chapter 4 is devoted to modelling and simulation of the Low-Voltage distribution network by focusing on the topology of the network and its effect on the capacity of the G3-PLC smart metering system.

The effect of topology on the performance of the system has been studied in Chapter 5, and the obtained results have been discussed.

The final chapter, Chapter 6, integrates the work and provides conclusions.

Chapter 2 : LITERATURE REVIEW

2.1. Introduction

The SG is the most used term for a power grid that is supported by a communication infrastructure. This communication network is used for monitoring and control of the grid's subsystems [16]. The SG is divided into seven domains as: i) Generation, ii) Transmission, iii) Distribution, iv) Customers, v) Operation, vi) Market and vii) Service providers [17]. The Generation, Transmission, Distribution and Customers domains are connected by bi-directional energy links. The Operation, Market, and Service provider domains, which are responsible for the grid management and supervisory and control applications, are communicating with the other domains using bi-directional flows of information.

The operation domain should respond to any changes that may happen throughout a grid, and therefore, the reliability and sustainability of a grid heavily depend on the timely transmission of data and control signals between different grid entities [18]. As a result, the communication network can be regarded as the backbone of the SG operation [19]. The AMI network is a part of the SG communication network that connects the grid's end-users to its back-end systems. Since many SG capabilities are realized through this part of the network, setting up an AMI is considered as a stepping stone towards the realization of the SG [20, 21].

The main component of an AMI network is the SM, which monitors a prosumer's consumption/production and can establish a bi-directional communication with the UCs' backhaul systems. SMs send information to the UC's data centres and receive commands and notifications from the UC's control servers [22]. Different SG applications can be implemented through this bi-directional flow of information, which can be beneficial to both UCs and consumers. From UCs' perspective, employing SMs reduces meters' reading costs and enables performing demand-side management through different mechanisms such as TOU. From the consumers' point of view, smart metering provides real-time consumption information, which can be displayed on interface units, such as in-home displays, internet portals or mobile applications. This enables consumers to effectively manage their consumption [23] by identifying energy-saving methods to save electricity consumption [24]. However, benefiting from the AMI in more advanced applications, such as limiting load, requires further considerations.

In this chapter, we first review the AMI network. This follows by covering AMI-based SG applications and their communication requirements. Thereafter, we review different technologies and standards used for developing AMI networks. Finally, an overview of the literature on modelling, analyzing and optimizing of PLC-based AMI networks have been covered.

2.2. Smart Metering Systems

The first generation of communicating meters is the automated meter reading (AMR) system. AMR systems operate based on one-way communication links, which connect multiple meters to a data centre and can only be used for remote data collection [25]. The collected data is used for billing, consumption analysis and troubleshooting purposes. Although employing AMR systems reduces labour costs and provides more accurate and up-to-date billing, it cannot be used in more advanced applications, such as demand response and load control applications.

The AMI is a developed version of AMR systems that benefits from SMs’ capabilities. SMs, which are more than just data collectors [12], make the AMI a sophisticated metering system capable of supporting data exchange between consumers and the UC. This technology opens up many new opportunities to increase the efficiency, reliability, and safety of the grid. Figure 2.1 depicts an overview of an AMI system. The AMI comprises SMs, DCs and meter data management systems (MDMS) [26].

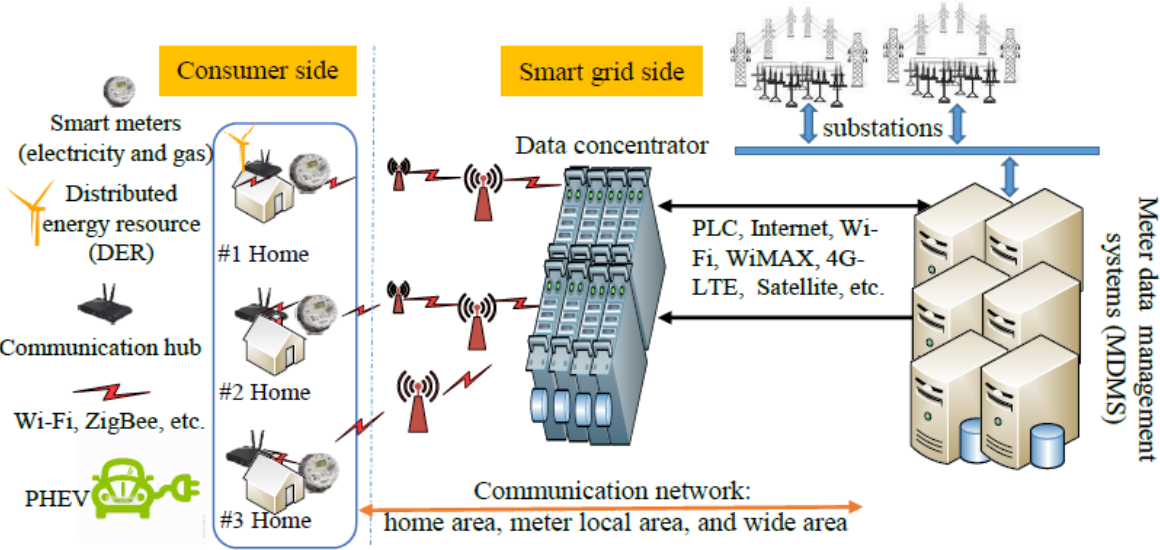


Figure 2.1. An AMI network and its components [27]

According to the IEEE2030-2011 standard, the AMI communication network is divided into three sub-networks: home-area network (HAN), neighbourhood-area network (NAN) and wide-area network (WAN) [28]. HAN links SMs to in-home smart appliances. NAN covers communications between SMs and DCs, and WAN consists of communication links between DCs and MDMS.

The consumer side of the AMI, or HAN, may consist of smart appliances, distributed energy resources, and different forms of energy storage units, such as plug-in hybrid electric vehicles (PHEVs). Data-rate required by each system may vary from 10 to 100 kbps [29]. An SM is a gateway to this part of the network, and its data traffic depends on the number and types of the connected devices.

An SM consists of a metering board and a communication board [30]. A metering board contains processing units and internal memories. The amount of consumed/generated energy together with other information such as values for voltage, current, frequency and power factor are measured and recorded by the meter board [31]. The metering section may consist of a real-time clock module to support services such as data analysis, billing, demand response and TOU pricing. A metering board is usually connected to a communication board using a serial port. A communication board is responsible for establishing a bi-directional communication link with a DC on the one side and with in-home appliances on the other side. Some SMs may also have a display unit for displaying power usage for billing and power monitoring purposes.

A DC collects measurement data at a set time interval. This part of an AMI network, which covers communication links between DCs and SMs, is known as NAN. DCs are gateways between NAN and WAN, and their function is to convert communication protocols and technologies between different parts of the network. In some AMI architectures, additional hardware such as data collectors and data aggregators may also be used between SMs and DCs. Such an architecture is especially common among wireless NANs.

A DC will forward the collected information to MDMS for further processing and storage [32]. Also, a DC conveys the control commands and notifications from the UC's control centres to the connected SMs. MDMS are the data centres used for the long-term storage of collected measurements and management of the events and data usages. MDMS consist of Outage Management System (OMS), Geographic Information System (GIS), Consumer Information

System (CIS) and Distribution Management system (DMS). MDMS analyse the collected data and assist with interaction between operational and managerial systems.

2.3. Communication Requirements for Potential Smart Metering Applications

The AMI's bi-directional communications capability provides an SG the opportunity to offer a variety of services, such as dynamic pricing, demand response (DR) [33], power quality monitoring, outage notification [34], theft detection [35] and remote power connection/disconnection [36]. A UC, for instance, can implement a demand response scheme by introducing TOU tariffs to achieve load reductions during peak hours. Also, the power outage and electricity theft detections can be obtained by analysing consumers' consumption information and detecting irregularities. Moreover, a demand-side management (DSM) service, as in the form of remote connection/disconnection of loads, can be implemented based on the remote-control ability of a smart metering system. The AMI can even help to integrate distributed generators into a power grid through providing access to real-time power consumption/generation information and enable remote-control of the distributed resources [37]. In the following sections, the communication requirements of the AMI network for different SG applications are discussed.

2.3.1. General Requirements

The scalability, interoperability and security are general requirements of an AMI network. The scalability refers to the capability of an AMI network to seamlessly accept new communication nodes such as meters, sensors, and data collectors [38]. Moreover, the communication backbone should be capable of handling the ever-increasing amount of collected data and new functionalities.

The interoperability is an important issue for UCs to reduce their costs. Old meters from one vendor should be replaceable by new meters from another vendor without the need to change software or hardware components. By adhering to specific standards and protocols, meters can communicate with one another regardless of their vendors. The interoperability can also be considered among different standards.

Data transmission and storage security is also crucial requirement as the collected data from SMs contains important information about customers. Moreover, the lack of security can expose the grid to fraud and sabotage [39], and adequate security needs to be established to prevent cyber-attacks.

2.3.2. Technical Requirements

Communication range, robustness, data-rate and latency are the technical requirements that should be considered in SG applications. Communication range is the maximum distance that information could be transmitted reliably. This criterion identifies the allowed distance between a transmitter and a receiver. Repeaters can be used to increase such ranges, although this will increase the cost of a network. A meter's location, for example, is directly affected by the communication range. If the plan is to locate a meter inside a building, a technology that can cover transmission over such a distance has to be selected.

The robustness requirement emphasizes on establishing an error-free communication between a transmitter and a receiver. Deploying suitable modulation and error-correction codes are among the techniques to reduce interference impairments and improve robustness in a system. Communication data-rate identifies the maximum information that can reliably be transmitted between transmitters and receivers. Such a requirement is directly related to the available frequency bandwidth. For interference control purposes, it is preferable to select a frequency band that can solely be available to a utility company. However, the frequency band exclusivity will only be achieved at a cost.

Latency is defined as the amount of time that will take for information to be transmitted between transmitters and receivers. Different SG applications have different latency requirements. Latency is a crucial factor in real-time applications such as DSM and micro-generation integration. Table 2-1 gives an overview of typical data-rate and latency requirements for common SG applications [40]. Greater data-rates can impose longer latency on a system. Therefore, a technology has to be selected in such a way to fulfil applications' data-rate and latency requirements.

Table 2-1: Overview of typical data-rate and latency requirements for different SG applications.

Application	Typical acceptable latency	Typical data-rate
Classical meter reading	10-60min	Hundreds of Bytes
Real-time metering	12-20 ms	Tens to Hundreds of Bytes
Protection	1-10 ms	Tens of Bytes
Control	100 ms	Tens of Bytes

2.4. Smart Metering Technologies and Standards

Different wireline and wireless technologies have been used in AMI networks. While wireless technologies are more suitable for geographically dispersed and versatile networks, PLC technologies are the most preferred in dense urban areas, as they do not require additional media installation and become more cost-effective [41]. A comparison between wireless and PLC technologies is given in Table 2-2.

Table 2-2: Comparison between using wireless and PLC technologies in the AMI

Technology	Advantages	Disadvantages
Wired (PLC)	<ul style="list-style-type: none"> - Cost-effective - Infrastructure owned by utility companies - Can be used in analysing grid infrastructure 	<ul style="list-style-type: none"> - Low data-rate - Complex routing - Noisy medium
Wireless	<ul style="list-style-type: none"> - Can be distributed regionally - Self-healing capability - High flexibility and self-forming capability 	<ul style="list-style-type: none"> - Requires additional infrastructure - Prone to external interference

2.4.1. Wireless Technologies

Wireless standards such as IEEE 802.15.4 (Zigbee and Zwave) and IEEE 802.11 have a great potential to be used in an AMI’s HAN [42]. IEEE 802.15.4 can establish low-cost, energy-efficient communication networks with data-rates of up to 250 kbps over a range of 50m. However, IEEE 802.15.4 does not contain a sufficient level of security [43]. IEEE 802.11, on the other hand, supports secure communication with data-rates of up to 54Mbps over a range

of 300m. Nevertheless, it is prone to interference and suffers from high power consumption [44].

The cellular and radio frequency (RF) mesh are the most used wireless technologies in the AMI's NAN [45]. Cellular technologies can offer high data-rate communication over long ranges; however, establishing cellular infrastructure owned by a UC is very costly. The required infrastructure can, alternatively, be hired from a cellular communications service provider. Nevertheless, this can bring in other concerns, such as reliability and security of the network. RF communication is the other type of wireless technologies, which is used in the AMI's NAN. RF links use unlicensed radio frequencies of up to 900MHz, which makes them vulnerable to interference caused by other transmitters operating in this band. Nevertheless, an RF-based NAN has the advantage of being self-formed and self-healed. This is because, the collected information by an SM is routed to a DC by hopping through other SMs, and if a meter becomes faulty, a different route can be established to get information across.

IEEE 802.16 (WiMAX) [46], IEEE 802.20 (MobileFi) and other cellular standards have been proposed for the AMI's WAN. Although in many countries wired technologies, such as fibre optic communications are more preferred for this part of the network [47]. The standards and technologies used for WAN should be capable of supporting high data-rate communication over a range of a few tens of kilometres.

2.4.2. Power-line Communication Technologies

PLC technologies use frequency modulation techniques for data transmission, and they are categorized, according to their operational bandwidths, into three major categories: Ultra-narrowband PLC (UNB-PLC), narrowband PLC (NB-PLC) and broadband PLC (BPL). UNB-PLC systems, which utilize frequencies below 3 kHz, can transmit information over long distances without a need for repeaters. However, UNB-PLCs are only useful for low data-rate transmissions. NB-PLCs, on the other hand, operate at the frequency range of 3 to 500 kHz. This frequency range includes the US Federal Communication Commission (FCC) band (10-490 kHz), the Japanese Association of Radio Industries and Business (ARIB) band (10-450 kHz), the Chinese band (3-500 kHz), and the European CENELEC bands: CENELEC-A (35.9-90.6 kHz), CENELEC-B (98.4-120.3 kHz), CENELEC-C (125-140 kHz) and CENELEC-D

(140-143.7 kHz). NB-PLCs can only support transmissions of up to 500 kbps. Lastly, BPLs operate at the frequency ranges of 1 to 250 MHz with data-rates of up to 500 Mbps.

The data-rate in PLC technologies reduces by the increase in transmission range. As a result, BPL systems have limited transmission range of few hundred meters. Moreover, BPL standards are not interoperable, which makes them a less favourable technology to be used in smart metering applications. NB-PLCs, on the other hand, are useful for smart grid’s supervisory, control and telemetry applications. NB-PLCs can cover a range of 2 km and in many countries like China, Britain, France, Italy and South Africa are the preferred technology to be used in the AMI’s NAN.

2.4.3. Standards

Smart metering systems, regardless of their employed communication technologies, should operate in accordance with data exchange standards. This allows seamless interoperability between different smart metering elements from different vendors [48]. Such interoperability reduces costs and opens doors to a larger market [49]. Governments, standard bodies and utility companies are the stakeholders involved in developing smart metering standards. However, despite their continuous attempts, no widely accepted standard for AMI applications exists, and unfortunately, the smart metering devices that are designed based on different standards cannot generally be integrated into one network. In this section, we review the most used standards of the AMI’s NAN, which is commonly considered as the most challenging layer of the AMI network. These standards are given in Table 2-3, where some are based on a specific technology, and others only cover the AMI’s data exchange protocols.

Table 2-3: Commonly used standards in the AMI’s NAN

Technology	Standard Name
Data Exchange	DLMS/COSEM, oneM2M
Wireless	GSM/GPRS, UMTS, LTE, MeshNet3, Flexnet, KamstrupRF, 802.15.4
PLC	PLAN, AMIS, Meter&More, OSGP, PRIME, G3-PLC, G.9902, 1901.2

During the European standardization process, it became clear that there is a need for a single application data model to help improving interoperability between devices and databases in an AMI network. Data exchange standards have been developed to serve such a need. The most

popular data exchange standard in smart metering applications is DLMS/COSEM [50-52]. However, in some wireless smart metering systems, the data modelling has been influenced by the concept of wireless sensor networks (WSN) and Machine-to-Machine communications [53]. An example of such data modelling can be seen in the OneM2M data exchange standard, where it aims to enable the Internet of things among different connected devices. OneM2M can be used in conjunction with IPv6 over Low Power Wireless Personal Area Networks (6LoWPANs) [54] and Routing protocols for low Power and Lossy networks (RPL) [55-57].

Cellular standards, such as GSM/GPRS, UMTS and LTE are among popular standards used in wireless AMI systems. The other group of standards used in wireless NAN are based on RF mesh technologies. KamstrupRF, MeshNet3 and Flexnet are examples of such standards. KamstrupRF and MeshNet3 can achieve data-rates of up to 9.6 kbps over a range of 10 km in rural areas. Flexnet, on the other hand, supports data-rates of up to 172 kbps over a range of 30 km.

As was mentioned before, AMI networks based on NB-PLC technologies are very popular, and different standards for such systems have been proposed and implemented around the world. NB-PLC technologies are categorized into two groups as low data-rate (LDR) and high data-rate (HDR). LDR NB-PLCs operate based on single carrier modulation and have a transmission rate of a few tens of kbps. Open Smart Grid Protocol (OSGP), Meters&More, Power Line Automation Network (PLAN) and Automated Measuring and Information System (AMIS) are the most popular LDR NB-PLC standards.

OSGP was initially promoted by Echelon and partially standardized by the International Electrotechnical Commission (IEC) under ISO/IEC 14908-3. OSGP has the highest penetration in Russia and Nordic countries. Another well-known LDR NB-PLC standard is Meters&More, which is widely used in Spain and Italy's AMI network. Meters&More is led by the ENEL group. Both OSGP and Meters&More standards use Binary Phase Shift Keying (B-PSK) modulation and can achieve data-rates of up to 57kbps. The other European LDR NB-PLC standard is PLAN, which is standardized by the IEC under IEC 61334 and is the most widely used LDR NB-PLC standard in South Africa. As a requirement by the European standards body CENELEC, PLAN should operate over the CENELEC-A band and so it can co-exist with other compatible standards on the same AMI network. AMIS is an LDR NB-PLC standard developed

by Siemens and uses Differential Code Shift keying (DCSK) to transmit data-rates of up to 3kbps. AMIS is mainly deployed in Austria.

HDR NB-PLC standards can offer higher throughputs (up to 1Gbps) by employing orthogonal frequency-division multiplexing (OFDM) modulation over a frequency range of 9 to 500 kHz. Power line intelligent metering evolution (PRIME) that is later standardized as ITU G.9904, G3-PLC (ITU G.9903), ITU G.9902 and IEEE 1901.2 are the most popular HDR NB-PLC standards for smart metering applications [58].

PRIME is proposed by Iberdrola, a Spanish distribution system operator, and has two versions. The European version, PRIME v1.3.6, operates over CENELEC-A frequency band and the American version, PRIME V1.4, which is designed for the frequencies of up to 500 kHz. PRIME v1.3.6 can transmit data-rates in the range of 21.4 to 128.6 kbps, and uses convolutional codes for error correction. PRIME can only support IPv4.

G3-PLC, which is developed by ERDF (a French distribution system operator) has a transmission rate in the range of 2.4 to 33.4 kbps over CENELEC-A frequency band, and can support up to 150 kbps over 150 to 500 kHz (FCC) band. It also supports IPv6. G3-PLC standard uses extensive channel coding techniques to increase data transmission robustness at lower data rate transmissions.

Interoperability is an issue among different NB-PLC standards. For example, PRIME standard cannot coexist with PLAN on the same network segment. However, G3-PLC and PLAN, which are the two standards used in South Africa are designed to be interoperable. The G3-PLC uses extensive forward error-correction (FEC) coding techniques, and therefore, it is more robust to the noise level on the DC compared to the PLAN standard. Although the raw data-rate for the G3-PLC is 15 times greater than the PLAN standard over CENELEC-A frequency band, the field test experiences show that the throughput measured at an application layer is around 4 times the throughput known for the PLAN. The G3-PLC works as an IP-based network and allows any-to-any communications. This is particularly useful for South Africa's prepaid meters that the inside house keypad, which is used for charging and reading the balance, has to communicate with the smart meter, which is mounted on a pole outside the premises.

There have been attempts by both ITU-T and IEEE to homogenize NB-PLC metering standards. ITU G.9902 (ITU-T G.hnem) is an attempt taken by ITU-T in this regard, which contains the recommendation for NB-PLC technologies over both CENELEC and FCC frequency bands. The focus of the ITU G.9902 is on robustness, which even outperforms G3-PLC. IEEE 1901.2 is an attempt by the IEEE to standardize NB-PLC technologies. It includes both PRIME and G3-PLC specifications with providing mechanisms that both standards can coexist on the same network. Table 2-4 summarizes the technical characteristic of the mentioned NB-PLC standards.

Table 2-4: An overview of the technical characteristic of the NB-PLC standards

Standard	Modulation	Data-Rates	Frequency Band	IP	Other features
PLAN	S-FSK	0.2-2.4 kbps	CENELEC-A		
AMIS	DCSK	0.6-3 kbps	CENELEC-A		
OSGP	B-PSK	3.6-57.6 kbps	CENELEC-A		
Meters&More	B-PSK	4.8-57.6 kbps	CENELEC-A, ARIB, FCC		
PRIME	OFDM	21.4-128.6 kbps	CENELEC-A	iPv4	Tree
G3-PLC	OFDM	2.4-33.4kbps	CENELEC-A, ARIB, FCC	iPv6	Robust mode, mesh routing
1901.2	OFDM	Approx. 80kbps	CENELEC-A, ARIB, FCC	iPv6	Coherent modulation
G.9902	OFDM	Approx. 80kbps	CENELEC-A, FCC	iPv6	Coherent modulation

It is a common practice to study the communication standards in the context of the layered network, especially according to the open system interconnection (OSI) reference model, which is the most widely used reference model for discussing layered networks. A comparison of the OSI reference model layer mapping of the standards given in Table 2-3 is shown in Figure 2.2.

Standards	PLC standards										Wireless standards						
	Application standards																
OSI Stack	P-LAN	1901.2	G.9902	PRIME	G3	AMIS	Meters & More	LON/OSGP	DLMS/COSEM	oneM2M	Meshnet3	Kamstrup RF	Flexnet	802.15.4	GSM/GPRS	UMTS	LTE
7 Application						AMIS	Meters & More	GS OSG 001	IEC 62056-6-2	based on ETSI TR 102 691	Meshnet3	Kamstrup RF					
6 Presentation						AMIS	Meters & More		IEC 62056-6-1		Meshnet3	Kamstrup RF					
5 Session						AMIS	Meters & More		IEC 62056-5-3		Meshnet3	Kamstrup RF					
4 Transport					UDP: IETF RFC 768	AMIS	Meters & More		TCP/IP IEC 62056-47		Meshnet3	Kamstrup RF					
3 Network					IPv6: IETF RFC 2460	AMIS	Meters & More	EN14908-1 (LONWorks)			IPv4	Kamstrup RF					
2 Data Link	IEC 61334-4-32	IEEE P1901.2	ITU G.9902	ITU G.9904 PRIME MAC	6LoWPAN Adaptation: IETF RFC 4944 + ITU G.9903 G3 MAC (based on IEEE 802.15.4-2006)	CX1	Meters & More (based on IEC 61334-4-32)	ISO/IEC 14908 (LONWorks)			Meshnet3	Kamstrup RF	Flexnet	IEEE 802.15.4e	GSM/GPRS	UMTS	LTE
1 Physical	IEC 61334-5-1	IEEE P1901.2	ITU G.9902	ITU G.9904 PRIME PHY	ITU G.9903 G3 PHY	CX1	Meters & More (CLC/prTS 50558-4)	ETSI TS 103 908 (modified 14908-3 LONWorks)			Meshnet3	Kamstrup RF	Flexnet	IEEE 802.15.4g	GSM/GPRS	UMTS	LTE

Figure 2.2. OSI layer mapping of AMI NAN standards [13].

As is seen, some of the standards, such as AMIS or MeshNet3, completely cover all the OSI layers, while the other standards such as the DLMS/COSEM and G3-PLC partially cover the layers. The DLMS/COSEM is used as an application layer for many smart metering standards including the G3-PLC, PRIME and PLAN. The approach in designing the DLMS/COSEM was to make sure that all AMI's functionalities are included in one standard.

2.5. Studies on the PLC-based AMI Networks

The PRIME and G3-PLC are the most widely used PLC-based standards in AMI networks. Both of these standards are categorized as HDR NB-PLC technologies and, at their physical

layers, benefit from OFDM and a variety of FEC techniques. The PRIME, which is supported by the PRIME Alliance, has been deployed on more than 20 million SMs across 15 different countries in the world [59]. On the other hand, the G3-PLC that is supported by the G3-PLC alliance has a larger market, and it is currently used by over 80 million products in more than 30 countries [60]. In this section, we review the literature on the research that has been made on modelling, simulation and improving the performance of the PLC-based AMI networks.

There are two approaches that have been considered in studying the PLC-based AMI networks. The first approach benefits from field tests on existing infrastructures. Such studies have been done on both AMI networks based on PRIME [61, 62] and G3-PLC [63, 64]. The other approach, studies AMI networks through simulations and analytical methods. [65-68] evaluated PRIME AMI networks through simulation, and [69] is an attempt to simulate G3-PLC networks. Analytical approaches can be useful in the sense that they can provide a fair network performance approximation prior to installing physical equipment. This helps to avoid any unnecessary costs due to the network alteration. The performance of some simulators has been tested against the data that was collected from field studies. SimPRIME [70] is an example of such network simulators, which has been developed to study the PRIME standard on AMI networks. In [71], the simulation results obtained from the SimPRIME have been compared against the data collected from field studies and showed that a well-designed simulator, such as SimPRIME, is a reliable tool in studying an AMI network.

Traditionally, the focus of much research in PLC-based AMI networks was to, first, model the physical layer of a standard and then attempt to improve its performance [66, 72, 73]. The work presented in [74] has attracted more attention among different studies that have been done on modelling the physical layer. In this work, the transmission line theory was used to model PLC channels with transfer functions. The obtained transfer function was then used to identify the frequency response of a PLC channel. The transmission line and the graph theories have been combined in [75] to propose an analytical approach for computing the signal attenuation in a PLC-based AMI network. In addition to the frequency-selectivity of a PLC medium, noise is also an important factor in PLC communications. Background noise [76] and impulsive noise [77] are the two major impairments in PLC channels. The model of the G3-PLC standard's physical layer is given in [78]. Also, the source of the noise in the G3-PLC network in the United States powerlines has been studied in [63]. For a PLC channel with variable load

connections, [79] proposed using the weighted random number generator concept for modelling the variations.

The performance of the MAC protocols in a PLC-based AMI network has been studied in [80, 81]. It was shown that the MAC layer protocols are required to be carefully adjusted to be suitable for being effectively used in the PLC-based networks [64]. A dynamic trust evaluation method is designed in [82] to improve the performance of the G3-PLC standard's MAC layer.

Network layer protocols also play an important role in the overall performance of AMI networks. The effectiveness of wireless network protocols for being used in the PLC-based AMI network has been studied in [83]. Data transmission latency and communication outage can significantly affect the QoS required for fulfilling AMI applications. As a result, QoS-aware routing protocols have to be employed in AMI communication networks. For this purpose, first, the required QoS for an AMI application has to be identified, and then the focus should be on the routing methodologies to achieve such a QoS. The examples of QoS requirements can be an acceptable delay, jitter and connection outage probabilities. There are many challenges in selecting efficient routing protocols for an AMI network. Firstly, routing for SG applications should be based on multiple QoS-aware routing that holds multiple constraints. The probabilistic dynamics of a grid is another factor that should be considered in developing QoS requirements [84].

Multi-hop message routing is a challenge in PLC-based AMI networks. In such systems, each SM also acts as a repeater for the other SMs to extend the network coverage [85]. As a result, the topology of a network has a significant effect on the routing reliability in a PLC network. In [85, 86], the effects of unforeseen changes of topology on the reliability of PLC networks have been studied, and the concept of single-frequency network transmission is presented for flooding of messages. [87] revised the issue of routing in PLC networks considering that the nodes are static and that their location is known a priori, meaning that nodes know the communication route, which is supposed to be taken. Therefore, the decision is with each SM to forward a received packet or not. Such routing algorithms are known as geographic routing in wireless communications. These kinds of routing algorithms have the advantage of finding the shortest routing path and close the gap between flooding. Low-power and lossy networks (RPL) routing protocols are proposed in [88] to address the requirements of networks characterized by low-power supplies in lossy environments. These protocols are based on

adaptive and reconfigurable network operations. [89] proposed a hybrid routing protocol that combines local agility and centralized control. The recent shift in improving routing in the G3-PLC is towards employing artificial intelligence methods [90, 91].

Similar to any other communication network, topology should have an effect on the performance of an AMI network. The locations of SMs in PLC-based AMI networks have been considered in [59] to obtain optimum routing algorithms. The optimization problems were constrained by energy consumption and transmission delays. [60] studied PRIME AMI networks and proposed a method to obtain the optimized location to install data acquisition points. In their study, the latencies related to the MAC layer have been considered. Their optimization problem was constrained by the QoS of the links and the cost of the system. The optimized location of SMs in PLC-based AMI networks were found in [92]. They proposed a stochastic geometry-based method. The AMI network considered in this research has a dynamic nature, and the optimization is done by forecasting the topology in the future.

OPNET, OMNeT++ and NS3 are amongst the most popular network simulators that have been used for simulating the AMI networks. For instance, OPNET has been used in [93] to simulate the performance of a PLC-based AMI network. SimPRIME, which was mentioned earlier in this section as a well-designed simulator, is designed by combining MATLAB and OMNeT++. In addition to the SimPRIME, there are other AMI network simulators, such as the ones proposed in [94, 95] for PRIME and in [69] for G3-PLC standard, that are designed using OMNeT++.

2.6. Summary

This chapter, first, provided an overview of smart metering systems and their applications. It then covered different technologies and standards that have been used, around the world, at different layers of AMI networks. Different PLC-based standards, as the most widely used medium for data transmission in AMI NAN, have been discussed. Finally, a literature review has been provided on the studies that have been made on modelling, analysing and improving the performance of the two most used NB-PLC standards: PRIME and G3-PLC. The review of the literature showed that no research has been done on the effect of topology on the performance of an AMI network operating based on the G3-PLC standard.

Chapter 3 : SMART METERING STANDARDS IN SOUTH AFRICA

3.1. Introduction

According to the SANS 62056-21 document, the minimum requirements that South Africa's AMI system should obtain is as follows:

- The capability to record active energy every 30 minutes. (reactive energy measurements are optional)
- The capability to import/export energy measurements
- The support for TOU tariffs (TOU includes peak, standard and off-peak as daily tariffs, weekdays and weekend as weekly tariffs and summer and winter as annual tariffs)
- The capability to detect and record meter tampering, power outages and voltage irregularities in the range of 5-15% of nominal voltage.
- The support for utilities' load management, including the capability of SMs for controlling the smart appliances based on utilities' request. This consists of connecting/disconnecting high consumption loads, such as an electrical geyser or a swimming pool pump.

Although SANS 62056-21 document does not suggest any technology or standard for the AMI network, ESKOM has selected DLMS/COSEM for the application layer and PLAN and G3-PLC for the lower layers in its currently established AMI network.

PLAN is an LDR NB-PLC standard, which operates based on S-FSK modulation and has a low transmission rate of between 0.2 and 2.4 kbps. Although PLAN is a suitable standard for classical meter reading, it cannot support more advanced applications with higher data rate requirements. G3-PLC can coexist with PLAN on the same network segment and supports 15 times greater data rates. It also uses extensive FEC coding techniques, and so is more robust than the PLAN standard to the level of noise on DCs. Moreover, G3-PLC is an IP-based network, which allows any-to-any communications. This is particularly useful for South Africa's prepaid meters that an inside house keypad has to communicate with the smart meter mounted on a pole outside the premises.

In this chapter, the specifications of DLMS/COSEM and G3-PLC are discussed. Figure 3.1 shows an overview of the protocols used in different layers of G3-PLC metering applications. The upper three layers are part of the DLMS/COSEM suite, and the four lower layers belong to the G3-PLC.

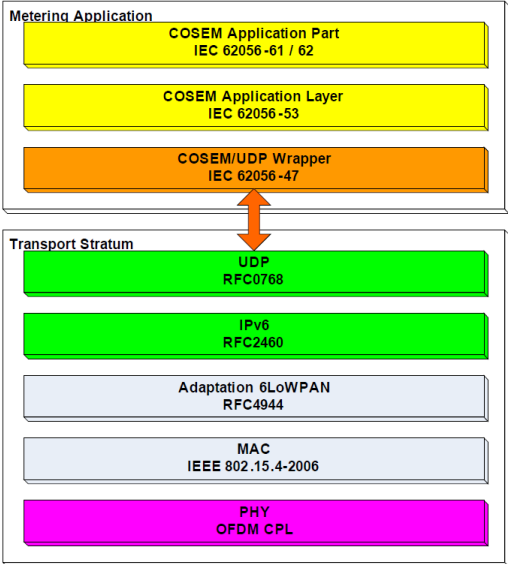


Figure 3.1. OSI layer mapping for metering application in G3-PLC

3.2. DLMS/COSEM

DLMS/COSEM is a suite of standards covering data exchange and interface modelling of metering devices. DLMS/COSEM has been amended by the IEC TC13 WG14 as IEC 62056 series of standards, specifically, for electricity metering applications [96]. Nevertheless, there are minor differences between the communication specifications of DLMS/COSEM and IEC 62056.

COSEM provides objective models for describing the functionalities of metering devices, and DLMS (IEC 62056-5-3) is a stack of open standards developed by the DLMS User Association (DLMS UA) for supporting data exchange for telemetry and remote control of different energy sources, including water, electricity, gas and heat. In other words, COSEM is the data model, which describes a meter’s functionality, and DLMS specifies the rules to access and modify (i.e., get/set) such data. DLMS/COSEM has been described by a set of colour coded

books (blue, green, yellow and white). Blue book describes the COSEM meter classes and interface object models. Green book covers DLMS’s architecture and protocol. Yellow book pertains questions concerning conformance testing, and white book contains glossary of terms.

G3-PLC employs COSEM interface classes (IEC 62056-6-2) and object identification system (IEC 62056-6-1) standards for interface modelling and data identification of AMI devices. According to IEC 62056-6-2, each physical metering device consists of a set of logical devices (LDs), where each LD supports one or more applications. For instance, in a multi-meter device, one LD can be allocated for the electricity metering, another for the gas metering and a third one for the water metering. Physical metering devices may have multiple LDs, but it is mandatory for every meter to contain a management LD. DCs, on the other hand, are modelled by a set of client application processes (APs) for representing metering functionalities. Similarly, a DC may have multiple APs, but it is mandatory for every DC to contain a public client AP. There are specific applications for the management LD and public client in establishing connections between meters and DCs, which will be explained later in this chapter.

The functionalities of LDs are defined through COSEM interface objects. A COSEM interface object is an instantiation of an interface class (IC). An IC is identified by a “class_id” and generalizes COSEM interface objects that share common characteristics. A COSEM interface object comprises of a set of attributes and methods for describing an LD’s functionalities. An LD may have one or more objects, but all LDs must have an “Association” object. This object has an attribute called “object list” containing the list of all available objects on an LD with their names, addresses and access rights. “Association” object would also be used in establishing communications between a DC and an LD.

COSEM interface objects are named with logical names (LNs). LNs are generated based on Object Identification System (OBIS), which is an octet-string of length 6 as

A	B	C	D	E	F
---	---	---	---	---	---

. The value of “A” identifies the energy type (A=1 for electricity related objects). The value of “B” is related to the channel number. The value of “C” depends on the value of “A” (Some of C values are given in Table 3-1 for A=1). The value of “D” identifies the method of measurements (e.g. instantaneous values, maximum value). The value of “E” refers to further measuring information, such as electricity fee (tariff rates), which is also identified according to the value of “A”. Finally, the value of “F” pertains historical information in a meter related to the parameters from “A” to “E”. More on the OBIS code values

can be found in the DLMS/COSEM blue book and the IEC 62056-6-1 standard. To reduce the complexity, it is also allowed to use the short names (SNs) mapped to the LNs.

Table 3-1: Value of group C for electricity energy (A=1)

Code	Physical data
0	General purpose objects
1	Active power+
3	Reactive power+
11	Current: any phase
12	Voltage: any phase
14	Supply frequency
⋮	⋮

An example of the COSEM model for an electricity meter capable of measuring active and reactive energy is shown in Figure 3.2. In this example, the “Register” IC with “class_id=3” is defined for modelling the generic register containing measured information. The “Register” IC has two attributes: “logical_name” and “value” and a method named “reset”. Two objects are instantiated from the “Register” IC for capturing the “Total Positive Active Energy” and the “Total Positive Reactive Energy”.

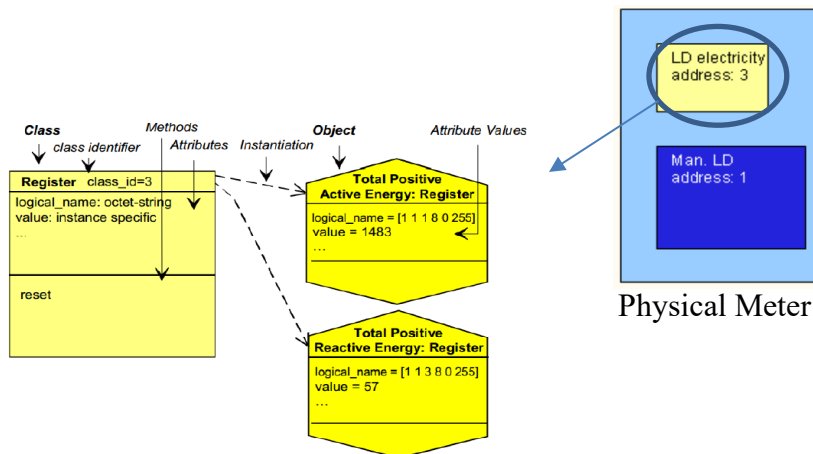


Figure 3.2. Example of COSEM object models

The DLMS protocol (IEC 62056-5-3) covers the data exchange between SMs and DCs. The communication follows a client/server model, where a DC acts as a client and the SM plays the role of a server. DLMS can be implemented on top of different lower layer protocols, including

Transmission control protocol (TCP) and User datagram protocol (UDP) at the transport layer, logical link control (LLC), High-Level Data Link Control (HDLC) and Medium access control (MAC) at the data-link layer and different PLC and RF technologies at the physical layer. DLMS is a connection-oriented protocol, which covers the logical connections between a client and a server and also the interconnections to the lower layers' protocols.

To establish a connection and collect data, the public client AP residing in a DC should communicate with the meter's management LD, also known as the server AP. The packet transfer by the DLMS protocol follows a precise sequence. This sequence is classified in three steps: namely set up data link, data transfer, and disconnect data link. Before data collection can take place, a communication link between client and server APs should be established. This is known as Application Association (AA) establishment, which is a logical connection between client and server APs and has to be supported by prior lower-layers connections. The association (logical connection) between APs is done by the Application Control Service Element (ACSE), which is an application layer's standard service. ACSE uses AARQ (A-Associate Request) and AARE (A-Associate Response) packets to start a connection. Once the AA established, data can be exchanged between a client and a server using another application layer standard service, known as the Extended DLMS application service element (xDLMS_ASE). The task of xDLMS_ASE is to access COSEM interface objects' attributes and methods. xDLMS_ASE uses the attributes of an LD's Association object, which are in the form of LNs or SNs, to identify and locate different objects residing in an LD. After the data exchange is complete, the session will be closed by releasing the AA. ACSE uses RLRQ (A-Release Request) and RLRE (A-Release Response) packets to terminate the session. The ACSE's application protocol data units (APDUs) are encoded by the basic encoding rule (BER), while the data transfers, which are done by xDLMS APDUs, are encoded in the Adapted extended data representation (A-XDR).

As was mentioned, the DLMS provides support for COSEM APs connections based on the services that receive from the lower layers. In G3-PLC, these lower layers are COSEM/UDP wrapper (IEC 62056-4-7), UDP, IPv4 or IPv6, which is implemented in conjunction with 6LoWPAN, MAC layer and finally OFDM PLC at the physical layer. Figure 3.3 shows an overview of the DLMS/COSEM, which is supported by the G3-PLC protocol.

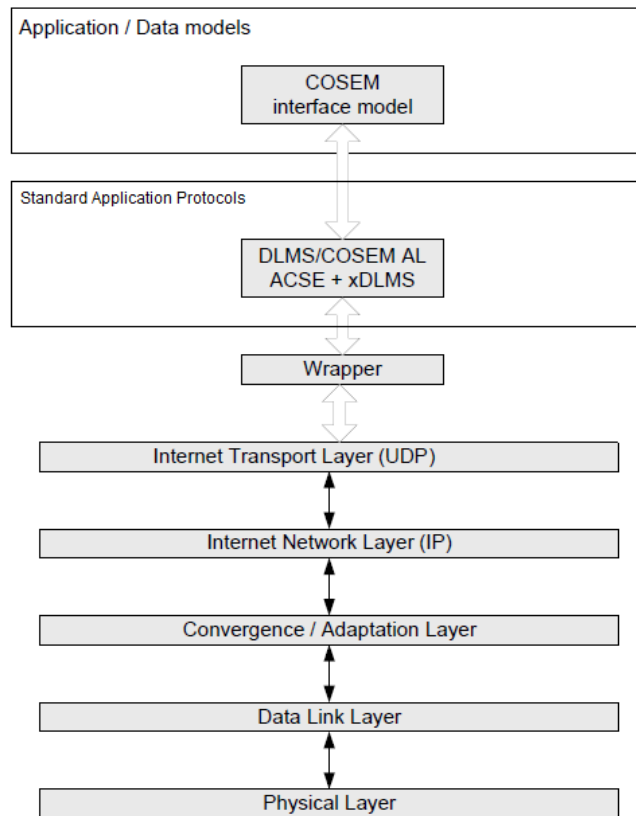


Figure 3.3. DLMS/COSEM supported by G3-PLC protocol

Addressing is an important part of any communication system. In a G3-PLC AMI network, an IP address is assigned to each physical device during the network registration process. Moreover, all LDs and APs are labelled by two-octets addresses known as Service Access Points (SAPs). While some SAPs are predefined, such as 0x10 for the public client APs and 0x01 for the management LDs, others are open to be assigned to other APs and LDs. Any new meter that is added to the network should first communicate with the DC’s public client AP to be registered. Also, a meter’s management LD contains SAP addresses for all the LDs residing in that meter.

The UDP wrapper (IEC 62056-4-7) task is to map the SAP values to a UDP port number, which is also known as the Wrapper port. The wrapper is a stateless protocol and only scales down the SAPs values to match the values of the UDP ports. The wrapper also helps with identifying the length of APDUs that are transmitted. The length of the payload will be included in the UDP header. The DLMS’s APDUs may consist of ACSE’s APDU or xDLMS APDUs with each has a different length. Therefore, there is a need for identifying the length of the packets.

3.3. Transport and Network Layer

The communication model of G3-PLC integrates a transport layer protocol with an IP suite in the network layer. The recommended network layer protocol for the G3-PLC is UDP (RFC 0768). However, UDP offers transport of datagrams in a non-connected mode, which is unreliable. To increase reliability, G3-PLC also allows the TCP protocol to be implemented at the transport layer. Nevertheless, TCP is not considered in the G3-PLC documentation, as sufficient reliability for data transmission have already been provided by subjacent layers.

For the network layer, both IPv4 and IPv6 have been considered by the standard. However, G3-PLC standard documentation considers IPv6 protocol (RFC 2460), which is preferred for supporting applications over the long term. The header size of UDP/IPv6 is originally 48 bytes. However, this amount of overhead would compromise the transmission speed. To overcome this problem, instead, G3-PLC uses compressed headers for the UDP and IPv6. The compression is done at the upper sublayer of data-link layer using an adaption sublayer, which will be covered in the next section.

3.4. Data-Link Layer

Data-link layer in G3-PLC consist of two sublayers: An adaption sublayer based on RFC 4944 and a MAC sublayer based on IEEE 802.15.4-2006. The adaption sublayer compresses the UDP/IPv6 headers. The compression is done by using 6LoWPAN (RFC 4944) specification. 6LoWPAN has been originally developed for supporting IPv6 on low-power devices with limited processing power. 6LoWPAN compresses the UDP/IPv6 headers from 48 bytes to 5 bytes.

Figure 3.4 shows the Adaption 6LoWPAN frame format. The number of the bytes for each frame segment has been shown above that frame segment. The HC1, HC2 and UDP sections are the 5 bytes, which represent the UDP/IPv6 header. HC1 and HC2 bytes are used to compress IPv6 and UDP headers, respectively. HC1 provides information on the compression format of IPv6, and HC2 byte holds information on UDP-header compression format. The byte that is shown as the IPv6 segment contains the Hop Limit value. The UDP component includes information about UDP source port, UDP destination port, the length of the UDP payload and

a checksum byte. The port numbers are compressed into 4-bit from their original 16-bit values. The actual 16-bit values are calculated by adding 0xF0B0 value to the compressed port number.

1	1	1	3	0-n
HC1 (IPv6)	HC2 (UDP)	IPv6 NC fields	UDP NC fields	Frame Body

Figure 3.4. The 6LoWPAN frame format for the G3-PLC

The routing function that the G3-PLC uses in the Mesh mode is the Lightweight On-demand Ad hoc Distance-vector (LOAD) protocol-next generation. LOAD is a simplified version of Ad-hoc On-demand Distance Vector (AODV) routing protocol that is drafted for 6LoWPAN. It is a reactive on-demand protocol, which means it is only triggered by the request of a source node and no periodic signalling is required. LOAD enables identifying the optimized route between any two nodes in a network. Optimization is done based on minimizing the route cost. The LOAD’s messaging diagram is shown in Figure 3.5.

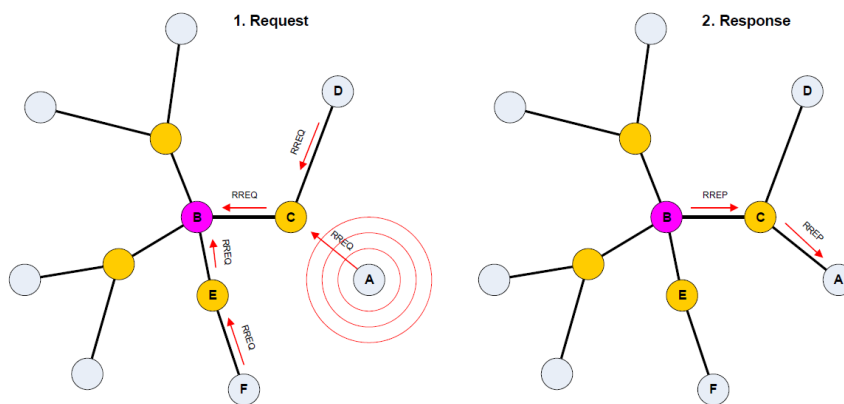


Figure 3.5. The messaging in LOAD protocol

When no valid route is available between a source and a destination node, the source node first broadcasts a route request signal (RREQ) to all its neighbouring nodes. RREQ carries route cost information based on the used metric. Each intermediate node on the path then adjusts the route cost information and forwards the signal to its neighbouring nodes till it reaches the destination. The destination can then select the optimized route according to the route cost information. The destination node will then unicast back a route replies (RREP) signal to the

source node. The source and intermediate nodes will be able to identify their neighbours and the optimal route through the RREP signal. The LOAD has originally been developed for the wireless network and has shown a few shortcomings in the PLC networks. As a result, an enhanced version of the LOAD for PLC networks has been developed. This enhanced version is known as the LOAD-next generation (LOADng) protocol.

To access the medium, the G3-PLC uses the carrier sense multiple access with collision avoidance (CSMA/CA) mechanism with a random back-off time. As a result of this random back-off mechanism, the collision probability will be reduced as the channel access time by a node is randomly spread over a period of time. After the back-off time is over, a node will try to access the medium. If the channel is found to be idle, the node starts transmitting. Alternatively, if the channel is found to be busy, the node shall wait for the next contention period based on the packet's priority. Then the process will start all over again by waiting for the back-off time to be expired before trying to access the channel.

A typical MAC layer data-frame is shown in Figure 3.6. As is seen, it encapsulates the 6LoWPAN frame by 13 bytes of header and 6 bytes of trailer. All segments except the security header and Message Integrity Check (MIC) are compulsory segments in every frame.

Bytes: 2	1	2	2	6	1	1	1	3	0-n	4	2
Frame Control	Seq Nbr	Dest PAN	Dest Addr (RA)	Security Header	HC1 (IPv6)	HC2 (UDP)	IPv6 NC fields	UDP NC fields	Frame Body	MIC	FCS

Figure 3.6. A typical MAC layer data frame

The Frame Control (FC) segment, which consists of 2 bytes, identifies the type of a frame and its format. This segment is followed by a byte of information on the sequence number, which is used to eliminate duplicate transmitted frames. The addressing is done by 4 bytes: Two bytes are considered for the PAN number to allow several networks coexisting on the same given infrastructure and two bytes for the destination address. The Security Header is optional and contains information related to the security methods and their information. The trailer has two segments: MIC and Frame Check Sequence (FCS). MIC is an optional but FCS is a compulsory segment. MIC length is four bytes and is used to verify whether the frame has been maliciously modified or truncated. FCS length is two bytes and is used to identify transmission disturbances during the frame transmission.

3.5. Physical Layer

G3-PLC has been defined over CENELEC, FCC, and ARIB bands. In this section, we look at the G3-PLC physical layer specifications defined over CENELEC-A band that has been used in South Africa. The frame structure of the G3-PLC at the physical layer is given in Figure 3.7. Each physical frame starts with a preamble sequence used for synchronization and detection in addition to automatic gain control adaptation. This sequence follows by a 5-bytes frame control header (FCH) block. The FCH contains important information that is required for demodulating the data frame. Figure 3.8 shows the overall block diagram of the transmitter in a G3-PLC system. The G3-PLC benefits from OFDM, differential phase shift-keying (DPSK) modulation and multiple FEC coding schemes to overcome harsh PLC channels' impairments.

	Bytes: 5	Bytes: 2	1	2	2	6	1	1	1	3	0-n	4	2
Preamble	Frame Control Header	Frame Control	Seq Nbr	Dest PAN	Dest Addr (RA)	Security Header	HC1 (IPv6)	HC2 (UDP)	IPv6 NC fields	UDP NC fields	Frame Body	MIC	FCS

Figure 3.7. A typical physical layer frame format

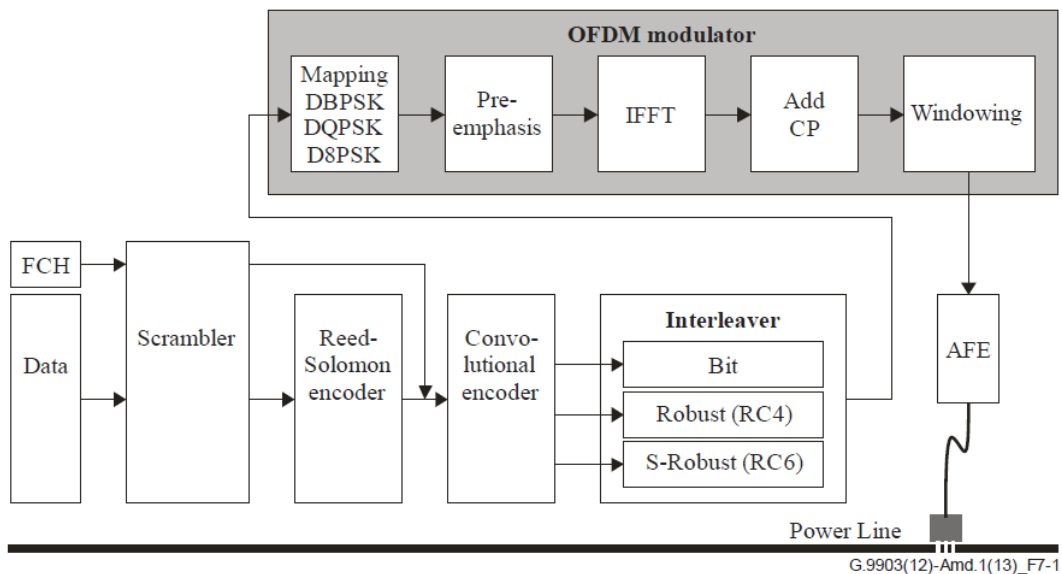


Figure 3.8. Block diagram of the G3-PLC transmitter at the physical layer

There are three modes of transmission in G3-PLC: Normal mode, Robust mode and Super Robust mode. Normal mode and robust mode are used for data transmission and super robust

mode is only used for transmission of the FCH. DBPSK is the modulation scheme for the robust and super robust modes, while the normal mode can use either DBPSK, DQPSK or D8PSK modulation schemes.

To transmit data across a PLC channel, the collected data from the upper layers, together with the 33 bits belonging to the FCH, should, first, go through a data scrambler block, which gives them a random-like distribution. The data bits are then encoded by shortened Reed-Solomon (RS) codes. The RS codes are either shortened from RS(255,247,8) or from RS(255,239,16). Shortening is done by making a certain number of data symbols equal to zero at the encoder and then re-inserting them at the decoder to be able to decode the codewords. The RS code rates used in CENELEC-A band is given in Table 3-2. The code rate selection is based on the chosen number of transmitted symbols per frame and the modulation scheme.

Table 3-2: RS encoders based on modulation

CENELEC-A Number of symbols	Reed-Solomon blocks (bytes) D8PSK (Out/In) (Note 1)	Reed-Solomon blocks (bytes) DQPSK (Out/In) (Note 1)	Reed-Solomon blocks (bytes) DBPSK (Out/In) (Note 1)	Reed-Solomon blocks (bytes) Robust (Out/In) (Note 2)
12	(80/64)	(53/37)	(26/10)	N/A
20	(134/118)	(89/73)	(44/28)	N/A
32	(215/199)	(143/127)	(71/55)	N/A
40	N/A	(179/163)	(89/73)	(21/13)
52	N/A	(233/217)	(116/100)	(28/20)
56	N/A	(251/235)	(125/109)	(30/22)
112	N/A	N/A	(251/235)	(62/54)
252	N/A	N/A	N/A	(141/133)
NOTE 1 – Reed-Solomon with 16 bytes parity.				
NOTE 2 – Reed-Solomon with 8 bytes parity.				

The encoded data and the FCH bits are then passed through two consecutive channel coding blocks: a convolutional code and a repetitive code (RC). The convolutional code has a rate of 1/2 and the constraint length of 7. The encoder is shown in Figure 3.9. The RC block code for super robust, robust and normal modes are RC(6,1), RC(4,1) and RC(1,1), respectively.

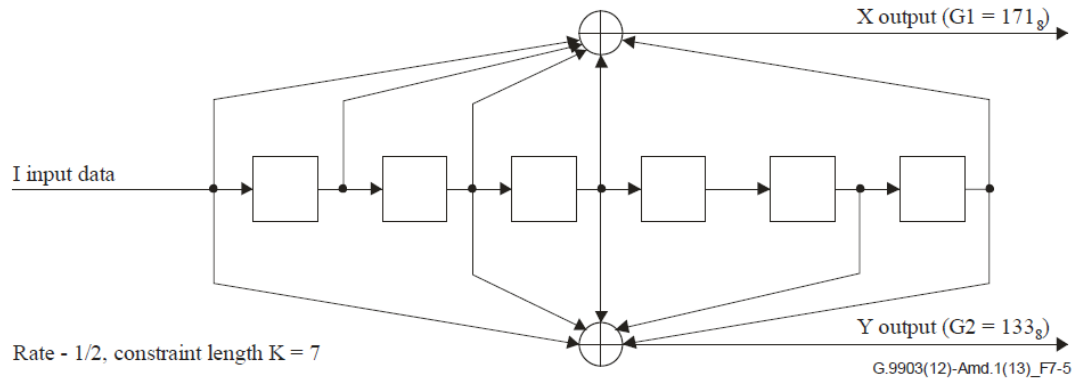


Figure 3.9. Convolutional encoder used in the G3-PLC

The G3-PLC uses a 256 points fast Fourier transform (FFT). In the CENELEC-A, only 36 subcarriers are active, and the rest are masked. Each subcarrier carries a DPSK modulated signal. DBPSK, DQPSK and D8PSK are the considered constellation sizes.

To prevent channel group delays, a 30-sample cyclic prefix (CP) is added to the beginning and again repeated at the end of each sequence. The generated sequence will then pass through a windowing block to reduce the out-of-band leakage of the transmit signals. Finally, the signal will be sent to the PLC medium through an analogue front-end (AFE)

To calculate the number of FCH symbols, we begin by considering $n_{FCH_bits} = 33$, which occupies 5 bytes. The output of the convolutional encoder contains

$$n_{FCH_bits_conv_encoded} = 2 \times (n_{FCH_bits} + 6) = 2 \times 39 = 78 \text{ bits} \quad (3-1)$$

The encoder adds six zero tail bits at the end of the input sequence to return the convolutional encoder to the "zero state". Since FCHs are transmitted in super robust mode, RC(6,1) will be used, and so the encoded sequence length of RC block encoder is

$$n_{FCH_bits_RC_encoded} = 6 \times n_{FCH_bits_conv_encoded} = 6 \times 78 = 468 \text{ bits} \quad (3-2)$$

and the number of OFDM symbols by considering that super robust mode uses DBPSK is equal to

$$n_{FCH_symbols} = \frac{n_{FCH_bits_RC_encoded}}{N_{carr}} = \frac{468}{36} = 13 \text{ symbols}$$

Therefore, in each physical frame, 13 OFDM symbols should be transmitted for the FCH. Also, the preamble length is 9.5 symbols.

Table 3-3 shows the achievable data-rate for different modulation schemes. The maximum data rate that can be achieved is by using RS (215,199) encoder. However, as is seen in Figure 3.7, 25 bytes of the header and trailer bytes should be transmitted in addition to the DLMS/COSEM payload. Therefore, the DLMS/COSEM payload transmission per physical frame is only 199-25=174 bytes, which makes its data rate equal to 37 kbit/s, considering sampling frequency of 0.4 MHz.

Table 3-3: Data rate for various G3-PLC modulation and coding schemes

CENELEC-A	Data rate per modulation type, bit/s			
	D8PSK, P16 (Note 1)	DQPSK, P16 (Note 1)	DBPSK, P16 (Note 1)	Robust, P8 (Note 2)
12	21 829	12 619	3 410	N/A
20	32 534	20 127	7 720	N/A
32	42 619	27 198	11 778	N/A
40	N/A	30 385	13 608	2 423
52	N/A	33 869	15 608	3 121
56	N/A	34 792	16 137	3 257
112	N/A	N/A	20 224	4 647
252	N/A	N/A	N/A	5 592

NOTE 1 – Reed-Solomon with a 16 byte parity.
 NOTE 2 – Reed-Solomon with an 8 byte parity.
 NOTE – N/A means not applicable and the reason for this is that the corresponding number of symbols specified results in an RS encoder block length that exceeds the maximum allowable limit of 255.

3.6. Summary

In this chapter, the specifications of the DLMS/COSEM and G3-PLC standard have been discussed. DLMS/COSEM is a suite of standards covering data exchange and interface

modelling of metering devices, and it can be implemented on top of different lower layer standards and technologies. The communication model of G3-PLC consists of the UDP/IP6 layer, RFC 4944 adaption layer, IEEE 802.15.4 MAC layer and an OFDM-based physical layer. We discussed the data exchange between SMs and DC. We also covered the format of data sequence at each layer of the G3-PLC standard. This provides a clear picture of the G3-PLC and its functionality.

CHAPTER 4 : MODELLING AND SIMULATION

4.1. Introduction

In this chapter, we provide the mathematical model of the system that will be used for studying the topology effect on the performance of the G3-PLC AMI network. In the G3-PLC based AMI network used in South Africa, SMs are located on the Low-Voltage (LV) lines and close to consumers' premises and should communicate with a DC that is installed on the secondary distribution transformer or inside a distribution cabinet. The focus of this work is on the residential distribution system. However, as the domestic loads are random in nature and vary with time, a statistical model for such loads is required.

The topology of the LV network could be affected by multiple factors, including the nature of the terrain, geographical location, the residential layout, cable sizes and types, and location of the transformer, among many other factors. For instance, in the USA, a smaller size transformer is used for a small number of houses, whereas in Europe, tens of residential loads are connected to a substation. In South Africa, the preferred transformer sizes are 25, 50, 100 and 200 kVA for Pole-mounted MV/LV transformers and 200, 315, 400, 500 and 630 kVA for the ground-mounted transformers. The transformers can be in three different forms as the three-phase, single-phase or bi-phase. Figure 4.1 depicts a typical LV distribution system. The fuses and circuit-breakers that are used for the overload protection of the system are shown by the square blocks. The fuse/circuit-breaker B, C, D, E and F are used to protect the LV busbar, LV feeder, service cable, the meter and consumer's distribution board, respectively.

The number of customers that are serviced by a transformer are calculated according to the transformer size and load model, knowing that the LV voltage level is 230V. Domestic electrical loads can generally be modelled as current sinks. It is not far from reality to consider the domestic load power factor close to unity, which makes the loads pure resistive. To provide a more accurate model for the loads, we consider a statistical probability function to describe the load, which will be covered in more detail in the following sections.

The PLC channel model in the AMI network can be significantly affected by the topology of the distribution network. A PLC channel can be modelled as a transfer function that is calculated according to the distance between different elements in the grid and the types of

cables that are used in the network. Both of these factors are directly related to the topology of the network.

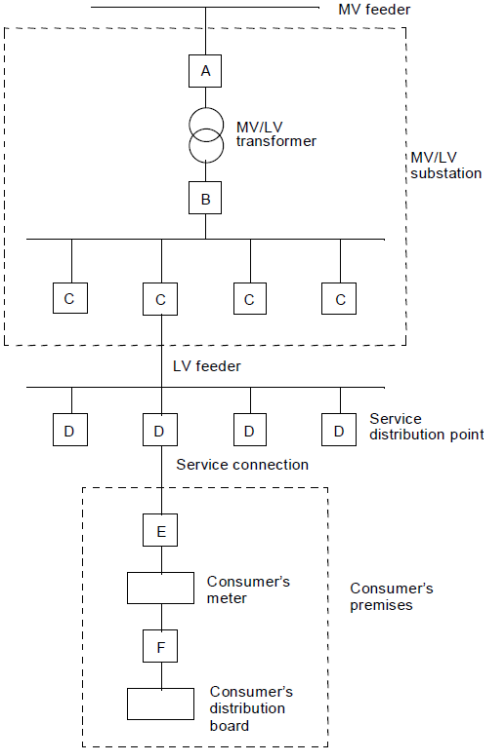


Figure 4.1. A typical LV distribution system

The final aspect that has to be considered in modelling a G3-PLC network is noise and disturbances effects. It will be shown that noise has a stochastic nature and is not affected by the topology of the network.

4.2. Load Modelling

The modelling of the loads causes the main source of uncertainty in the LV distribution system. The loads’ uncertainties can be modelled based on the probabilistic approaches, and in fact, studies have shown that the probabilistic approaches are suitable for modelling the Southern African LV consumers’ consumption. Moreover, analysis of the collected load data from South Africa supports the hypothesis that the residential electrical loads may be represented as constant current sinks. As a result, loads will be measured in amperes rather than kilovolt amperes or kilowatts. Heavy loads frequently have a substantial resistive heating

component, which results in a load power factor of around 1. Therefore, it is appropriate to assume that residential loads are current sinks with a power factor of one.

A statistical strategy is essential for a more precise description of the load. Statistical probability functions for diversified loads have been developed based on observing the consumption over a period of time. This follows by obtaining a histogram of the measurements in the form of occurrence frequency versus current. Then a probability density function (pdf) is selected to best describe the measurements' histogram. The Gaussian or normal pdf is more common for describing a large number of loads, and the skewed pdf, such as the Beta distribution, as is shown in Figure 4.2, is more appropriate for modelling current sinks in the LV distribution networks.

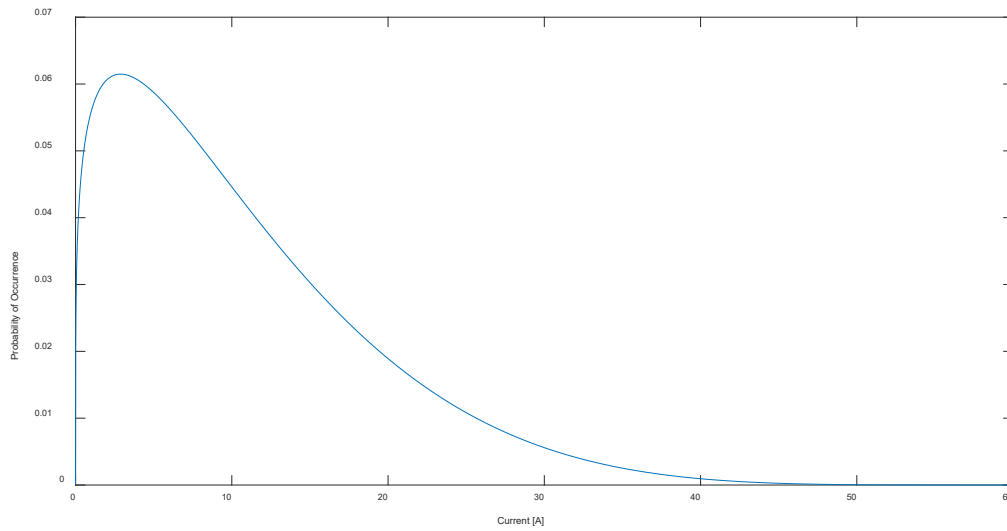


Figure 4.2. Typical load distribution for urban residential sector

According to Eskom data [97], the load distribution for the urban residential sector can be modelled as

$$f(i) = \frac{60}{B(1.23,5.56)} i^{0.23} (1 - i)^{4.56} \quad (4-1)$$

where B denotes the beta function. The mean value of this distribution is 10.9A. Although based on the average consumption, a 200kVA transformer can support 80 consumers, we consider an LV network comprised of 50 consumers connected to a 200KVA transformer considering the overload protection on the network. Moreover, NAYY150SE cable type has been considered for connecting loads to the transformer. This is a common cable type used in LV distribution

systems. The input impedance of each load is a function of the operation frequency. The average load impedance at 50 Hz, according to Figure 4.2 for the considered LV network, is 21Ω . Nevertheless, the input resistance of the G3-PLC modem is designed to be greater than 50Ω . When the modem resistance is applied in parallel to the 21Ω , the input impedance at the meter can be taken as 15Ω .

4.3. PLC Channel Model

From the communications perspective, two approaches have been used to model the PLC channels, commonly known as the top-down and bottom-up approaches. In the top-down approach, the PLC medium is considered as a multi-path channel, and its frequency response is calculated based on multi-path propagation theory as [77]

$$H(f) = \sum_{i=1}^N g_i e^{-\alpha(f)l_i} e^{-2\pi\tau_i} \quad (4-2)$$

where

- f is the transmitted signal frequency.
- N is the number of propagation paths.
- g_i is the transmission coefficient or the gain of the path i .
- α is the attenuation factor which is a function of frequency.
- l_i is the length of path i .
- τ_i is the propagation delay for path i .

This approach requires knowledge of the characteristic values of each path, which are the transmission, attenuation and propagation delay coefficients. These characteristic values are obtained by measurement and training data. Therefore, no prior information on the topology or the sizes and types of conductors used in the network is required. The top-down approach has been extensively used in literature. However, for obtaining an accurate model for a PLC channel, the computational complexity of this approach is relatively high. For instance, accurate modelling of a 110m long cable should be based on at least 44 paths [77]. Despite the popularity of the top-down approach, this model is not suitable for our study as it cannot predict the channel behaviour with respect to the change in the network topology.

The bottom-up approach, on the other hand, uses the transmission line theory and the two-port networks' method to obtain the frequency response of a PLC channel. In this approach, the conductor properties are used to calculate the impedance between any two nodes in the network. An equivalent circuit of a PLC channel between T and R nodes can be represented by a two-port network, as is shown in Figure 4.3.



Figure 4.3. A two-port network

The relation between the voltage and current at the transmitter and receiver is obtained by the ABCD parameters as

$$\begin{pmatrix} V_T \\ I_T \end{pmatrix} = \begin{pmatrix} A & B \\ C & D \end{pmatrix} \begin{pmatrix} V_R \\ I_R \end{pmatrix} = \mathbf{T} \begin{pmatrix} V_R \\ I_R \end{pmatrix} \quad (4-3)$$

The ABCD matrix is denoted with \mathbf{T} . The transfer function of the PLC channel between the two nodes is obtained as

$$H(f) = \frac{V_R}{V_T} = \frac{V_R}{AV_R + BI_R} = \frac{Z_R}{AZ_R + B} \quad (4-4)$$

where Z_R is the receiver node's input impedance that is also known as the end-line impedance.

The access impedance is the impedance value from the perspective of the transmitter to access the receiver. The access impedance of Z_R from the perspective of T in the circuit given in Figure 4.3 is equal to

$$Z_{Z_R:T} = \frac{V_T}{I_T} = \frac{AV_R + BI_R}{CV_R + DI_R} = \frac{AZ_R + B}{CZ_R + D} \quad (4-5)$$

The \mathbf{T} matrix of a transmission line can be calculated as [75]

$$\mathbf{T} = \begin{pmatrix} A & B \\ C & D \end{pmatrix} = \begin{pmatrix} \cosh(\gamma l) & Z_0 \sinh(\gamma l) \\ \frac{1}{Z_0} \sinh(\gamma l) & \cosh(\gamma l) \end{pmatrix} \quad (4-6)$$

where

l is the conductor length.

γ is the propagation constant of the line.

Z_0 is the characteristic impedance of the line.

The propagation constant and the characteristic impedance of the line can be obtained by

$$\gamma = \sqrt{(R + j2\pi fL) \times (G + j2\pi fC)} \quad (4-7)$$

and

$$Z_0 = \sqrt{\frac{(R + j2\pi fL)}{(G + j2\pi fC)}} \quad (4-8)$$

where

f is the transmitted signal frequency.

R is the amount of resistance per unit length of the line.

C is the amount of capacitance per unit length of the line.

L is the amount of inductance per unit length of the line.

G is the amount of admittance per unit length of the line.

For the selected NAYY150SE cable, $L = 0.33 \mu H/m$, $C = 0.27 pF/m$, and the values of R and G , are neglectable in the analysis [98]. As is seen, from equations (4-4) to (4-8), the ABCD parameters and hence the obtained transfer function of a transmission line depend on the electrical characteristic of the conductor. Therefore, this approach provides accurate results only if the cable parameters are known. However, these parameters are usually provided according to a test condition, and so the cables' aging and deviation from the test condition would affect the model accuracy. Nevertheless, the bottom-up approach provides a more suitable model for studying the topological effects in an LV network. Figure 4.4 presents the obtained transfer function for NAYY150SE cable in the range of the CENELEC-A band and

for three different cable lengths, showing the effect of the cable length on the value of the obtained transfer function.

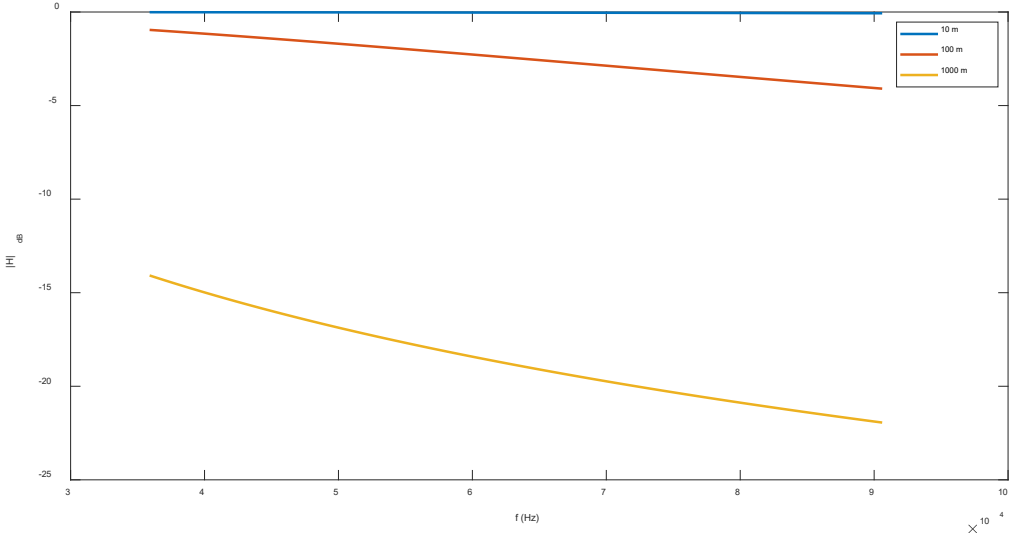


Figure 4.4. Transfer functions for the cable link of different length in the CENELEC-A band

The bottom-up approach can easily be applied to an LV distribution network to find the transfer function between any two nodes. A typical LV distribution network topology, as is shown in Figure 4.5, consists of a set of nodes (N), branches (B), and loads (Z). The T matrix for a branch can be calculated using equation (4-6). However, before being able to calculate the T matrix between any two nodes of a network, we need to be familiar with some properties of the bottom-up approach.

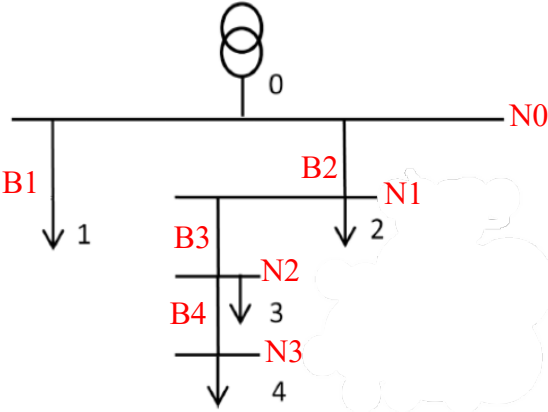


Figure 4.5. A simple LV distribution network

Property 1- For an end-load, Z_n , the T matrix is equal to

$$\mathbf{T}(Z_n) = \begin{pmatrix} 1 & 0 \\ \frac{1}{Z_n} & 1 \end{pmatrix} \quad (4-9)$$

Property 2- For cascade sections of a network, the equivalent T matrix is equal to the multiplication of T matrices of each section. For instance, the T matrix between the N_0 and N_1 , $T_{0,1}$, in Figure 4.6 can be obtained as $T_{0,1} = \mathbf{T}(B_1)\mathbf{T}(B_2)$, where $\mathbf{T}(B_1)$ and $\mathbf{T}(B_2)$ are calculated using (4-6).

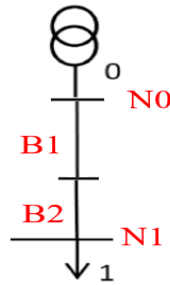


Figure 4.6. A simple two segment network

Property 3- The equivalent T matrix for parallel paths is obtained by calculating the access impedances of parallel branches and using Property 1. For instance, the T matrix between N_0 and N_1 in Figure 4.7 can be obtained as $T_{0,1} = \mathbf{T}(Z_{Z_1:N_0} || Z_{Z_3:N_0})\mathbf{T}(B_2)$, where $Z_{Z_1:N_0}$ and $Z_{Z_3:N_0}$ are the access impedances of Z_1 and Z_3 from the perspective of N_0 , respectively. Moreover, $Z_{Z_1:N_0} || Z_{Z_3:N_0} = \frac{Z_{Z_1:N_0} \times Z_{Z_3:N_0}}{Z_{Z_1:N_0} + Z_{Z_3:N_0}}$ is the equivalent impedance, and $\mathbf{T}(Z_{Z_1:N_0} || Z_{Z_3:N_0})$ is calculated from (4-9).

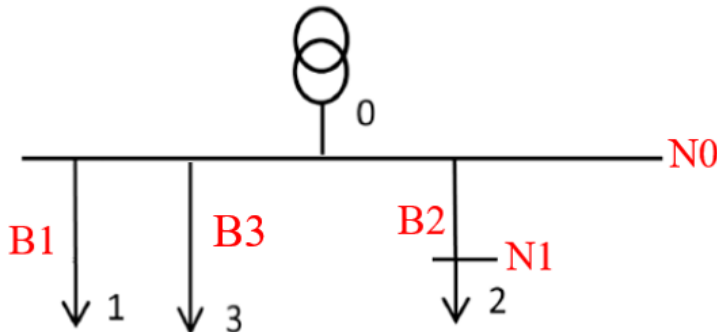


Figure 4.7. A simple network with parallel paths

Using these three properties, enable us to calculate the \mathbf{T} matrix between any two points in a network. For instance, the \mathbf{T} matrix between N_0 and N_2 in the network given in Figure 4.5 is equal to $\mathbf{T}_{0,2} = \mathbf{T}(Z_{Z_1:N_0})\mathbf{T}(B_2)\mathbf{T}(Z_2)\mathbf{T}(B_3)$.

4.4. Noise and Disturbances in NB-PLC

PLC channels are hostile media, which are affected by a variety of noise and disturbances. The main source of disturbance in PLC channels is due to Non-Intentional Emissions (NIE), which are generated by different electrical devices connected to an electrical grid. This problem has been identified by CENELEC and is addressed by the two amendments added to IEC 61000-2-2 for limiting the emission from non-communicating devices [99]. Noise in PLC channels, on the other hand, has a stochastic behaviour and is classified into background and impulsive noise.

Background noise refers to a type of noise that is always present and changes slowly with time. The background noise in PLC channels is in the form of coloured noise and narrowband interference. Coloured noise is produced by combining multiple noise sources, such as hair dryers, dimmers or computers, all of which may induce disruptions in the frequency range of 0-100MHz [100, 101]. The behaviour of the coloured noise varies according to the frequency, and so its power spectrum density (PSD) is frequency selective instead of flat. Therefore, coloured noise is commonly modelled as a frequency-dependent, low-power spectral density. The PSD of the coloured noise is usually given as [4]

$$S_{nb}(f) = a + be^{-cf} \quad \left[\frac{dBm}{Hz} \right] \quad (4-10)$$

where a, b and c are derived from channel observation through measurements, and f is the frequency in MHz. Narrowband interference consists of narrowband amplitude-modulated emissions generally caused by external broadcast radio bands. Narrowband interferences can be incorporated into the coloured noise model at certain frequencies to obtain the complete background noise model.

The impulsive noise in PLC channels consists of the harmonic and aperiodic components. The harmonic impulsive noise has two parts. One part is synced with the power supply

frequency, which is often caused by the silicon-controlled rectifiers (SCR) in a power supply and is synchronous with 50/100 Hz. The other part is as a result of the switching power sources that exist in a variety of home appliances, and their frequency ranges from 50 kHz to 200 kHz [102]. The aperiodic impulsive noise, on the other hand, is erratic in nature, owing to the transients due to the coupling and decoupling of electrical equipment.

The overall impulsive noise is modelled by an arrival process described by the statistics of its duration, amplitude and interarrival time. The majority of the impulsive noise models are based on amplitude statistics, including Middleton's electromagnetic interference classification [103] and the two-term Gaussian mixture model [104]. Although other models, such as the Markov chains [105], Bernoulli process [106] and curve-fitting techniques [107], have been used to model the impulsive noise, [108] showed that the channel's impulsive noise could be well modelled based on an approximation on Middleton's model as

$$P_{imp}(n) = \sum_{k=0}^2 \frac{e^{-5.8}(5.8)^k}{k!} \cdot \frac{1}{\sqrt{2\pi\sigma_k^2}} \exp\left(-\frac{n^2}{2\sigma_k^2}\right) \quad (4-11)$$

$$\sigma_k^2 = 10 \left(\frac{k}{5.8} + 0.1 \right) \sigma_b^2$$

which is a summation of three zero-mean Gaussian distribution. Therefore,

$$P_{imp}(n) = \frac{1}{\sqrt{2\pi(0.0124)\sigma_b^2}} \exp\left(-\frac{n^2}{2(0.0124)\sigma_b^2}\right) \quad (4-12)$$

$$\sigma_b^2 = 30 \int_{f_1}^{f_2} 10^{[S_{n_b}(f)-30]/10} df \quad [V]$$

assuming that the receiver input impedance is 15Ω.

It is common to consider a flat PSD for the noise in LV distribution networks' PLC channels for investigating the effect of topology in such networks. This practice is based on the fact that the noise is a common factor between all the nodes in a network [98]. Background noise PSD is usually considered around -145 dBm/Hz. Also, the amplitude of the impulsive noise is considered to be 40 dBm/Hz higher than background and narrowband noise as is reported in [109]. Therefore, in this study, we consider a flat PSD at -110 dBm/Hz for the receiver-side

noise, which is a relatively high noise. The PLC modems are assumed to transmit signals with a PSD of -55 dBm/Hz [110].

4.5. Channel Capacity

The channel capacity between the transmitter (node 0) and a receiver (node i) in the network can be calculated as

$$C_i = \int_{f_1}^{f_2} \log_2 \left[1 + \frac{S_i(f)}{N(f)} \right] df \quad (4-13)$$

where the transmitted signal frequency range is in $[f_1, f_2]$. $S_i(f)$ and $N(f)$ denote the PSD of the received signal and noise at node i . Based on the assumptions that both noise and transmitted signal have flat PSD, the capacity is equal to

$$C_i = \int_{f_1}^{f_2} \log_2 [1 + \overline{SNR} |H_i(f)|^2] df \quad (4-14)$$

where $\overline{SNR} = -55 - (-110) = 55$ dB and $H_i(f)$ is the transfer function between DC and node i (smart meter i). Therefore, in this research we use

$$\sum_i \left| \int_{f_1}^{f_2} H_i(f) df \right|_{dB} \quad (4-15)$$

as an indicator to compare the topologies' performance.

4.6. Topology Modelling

In this section, the approach for modelling the topology of the LV network in an urban area is discussed. The topology of the LV network could be affected by multiple factors, including the nature of the terrain, geographical location, the residential layout, cable sizes, and types and location of the transformer, among many other factors. A typical example of an urban layout is shown in Figure 4.8 (a), with its LV network topology given in Figure 4.8 (b).

As is seen, an LV distribution network can be modelled as a rooted tree, which is an acyclic connected graph. Any two vertices in a tree are connected by only one path. A path consists of one or more edges. The root of the tree is the vertex that has no parent, and the leaves of the tree are the vertices with no children. The degree of a vertex is equal to the number edges connected to that vertex. The height of a vertex is equal to the maximum number of edges in a path from that vertex to a leaf, and the depth of a vertex is the number of edges in its path to the tree root. Therefore, in an AMI network modelled by a tree graph, the DC is the tree root and the meters are the vertices. The PLC transmission lines form the edges of the tree.

We consider a residential layout, given in Figure 4.9, to obtain a general model, which is not constrained by the terrain or geographical location. The model consists of 50 houses that are uniformly spread in a $225 \times 225\text{m}^2$ area. All the houses are supplied by a transformer, which contains the DC. Based on graph theory, we can have $(50)^{50} - (49)^{50} - 1$ unique ways of connecting the houses to the transformer.

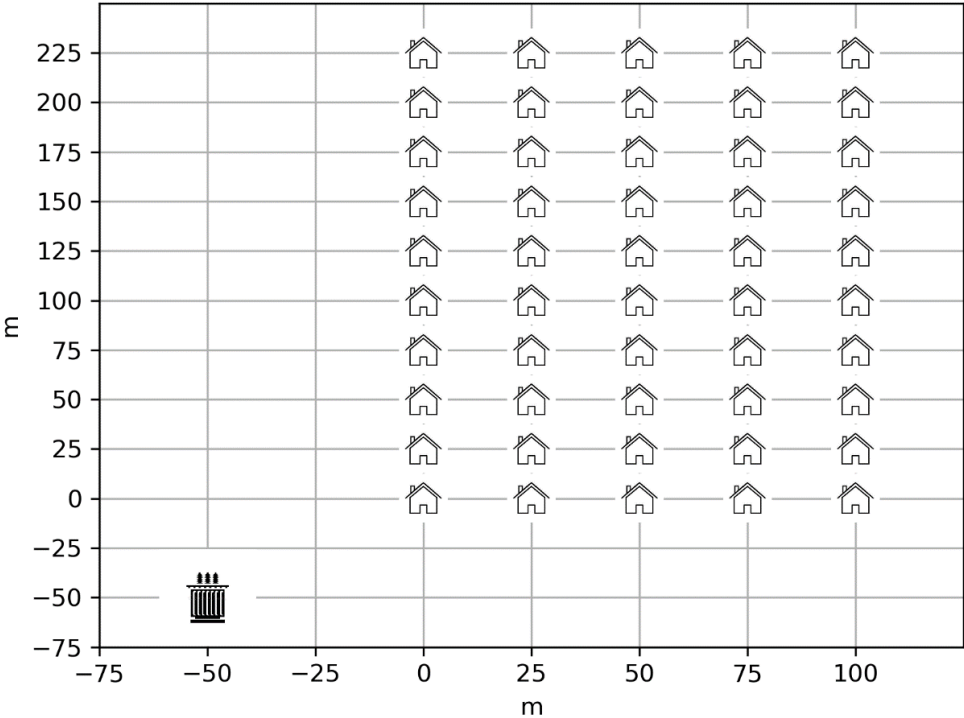


Figure 4.9. The model of the residential layout considered to study the topological effects

We used labelled trees to model the network, with the root labelled as zero and the meters labelled as 1 to 50. Therefore, the adjacency matrix for representing a tree graph for such AMI network is a 51×51 . The ij^{th} element of such a matrix is 1 if an edge connects node label i to node label j , otherwise it is equal to zero. An example of a pseudocode for generating a random given adjacency matrix is given in Figure 4.10.

```

for (i,j) = (1,1) to (50,50)
  Set a(i,j) = 0
UM = 50           #Number of unallocated meters
AM = 0           #Number of allocated meters
NL=0             #Node label
while UM > 0:
  M = randi(1,UM) # randi(1,UM) generates a random integer in [1,UM]
  for j= 1 to M
    Set a(NL,j) = 1
    Set a(j,NL) = 1
  AM = AM+M
  UM = UM - M
  NL = NL + M

```

Figure 4.10. The pseudocode for generating a random topology for the AMI network

4.7. Calculating Channel Transfer Function

In this section we provide an algorithm to calculate the transfer function between DC and meter i in the AMI network. The pseudocode for calculating $T_{0,i}$ in Figure 4.11.

```

T = 1
N=Set of all nodes in path 0 to i
for n in N
  if n==i
    T = T × T(Zi)
    break loop
  end if
  if degree(n) > 2
    M = Set of all leaves connected to n and not equal to i
    Yeq=0
    for m in M
      Yeq = Yeq + 1/ZZm:n
    end for
    T = T × T(1/ Yeq) × T(Bn-1->n)
  else
    T = T × T(Bn-1->n)
  end if
end for

```

Figure 4.11. The pseudocode for calculating $T_{0,i}$ between the DC and meter i

4.8. Summary

In this chapter, the mathematical model of the system used to study the topology effect on the performance of the G3-PLC AMI network was derived. We began by modelling the consumption load to identify a realistic model for the number of meters connected to a DC and the type of suitable cable for being used in the model. It was discussed that between the two approaches that have been used for modelling the PLC channels, the bottom-up approach is more suitable for studying the topological effects. We proposed an indicator based on the capacity of the overall AMI network to be used for comparing the performance of each topology. For this purpose, the noise model and the capacity of the channel in accordance with the G3-PLC standard have been studied. Moreover, we proposed a method to realistically model and simulate the topologies for the AMI network. Finally, an algorithm has been proposed to calculate the transfer function between different nodes in the network.

Chapter 5 : RESULTS AND DISCUSSIONS

5.1. Introduction

In this chapter, four different topologies have been considered and their performance has been compared. Three of these topologies have been used in the LV distribution network. Moreover, we consider a random topology to provide a better insight to the problem.

5.2. Sequential Topology

The first topology that is considered is in a sequential form, where the meters are connected in a sequence according to their geographical location. The layout of this topology and its corresponding tree graph are given in Figure 5.1 and Figure 5.2, respectively.

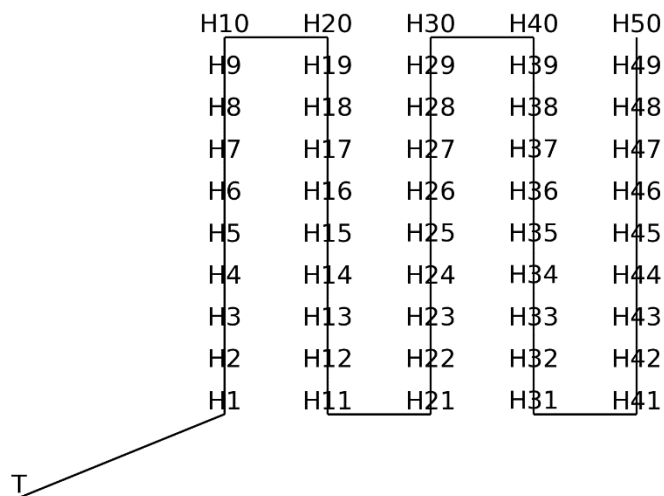


Figure 5.1. The considered sequential topology

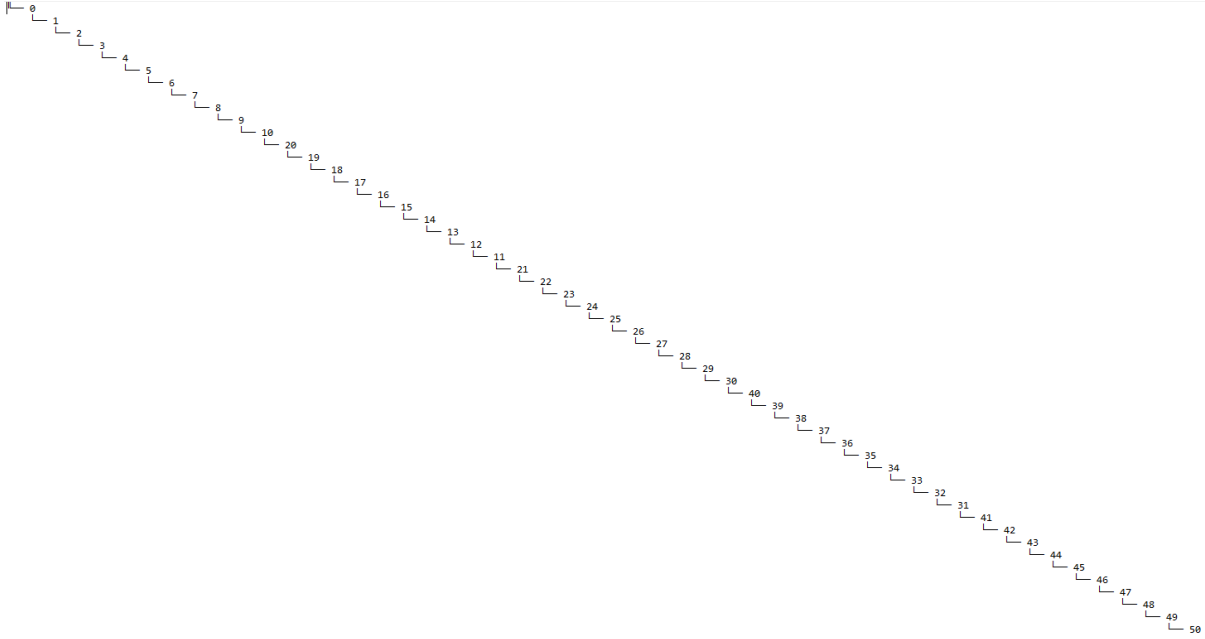


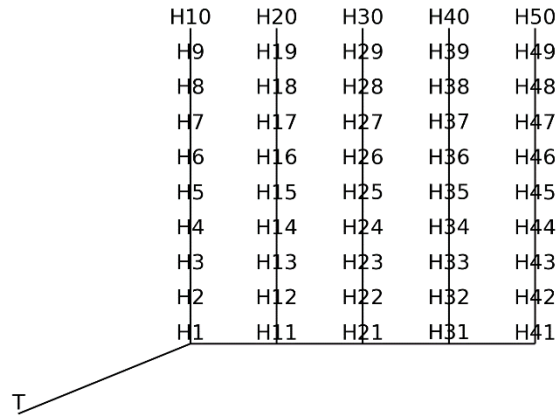
Figure 5.2. The tree graph for the considered sequential topology

For calculating the transfer function between every meter and DC, the resistance value at each node has been calculated as follows, where Z_i is the resistance of the load connected to node i and $Z_j: i$ is the resistance of node j from the perspective of node i .

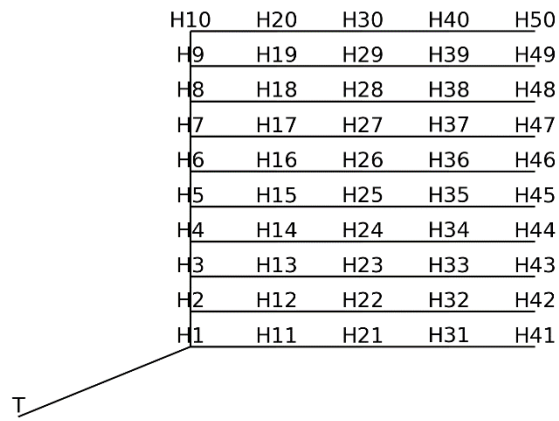
1 : (Z1) (Z2:1)	18 : (Z18) (Z17:18)	35 : (Z35) (Z34:35)
2 : (Z2) (Z3:2)	19 : (Z19) (Z18:19)	36 : (Z36) (Z35:36)
3 : (Z3) (Z4:3)	20 : (Z20) (Z19:20)	37 : (Z37) (Z36:37)
4 : (Z4) (Z5:4)	21 : (Z21) (Z22:21)	38 : (Z38) (Z37:38)
5 : (Z5) (Z6:5)	22 : (Z22) (Z23:22)	39 : (Z39) (Z38:39)
6 : (Z6) (Z7:6)	23 : (Z23) (Z24:23)	40 : (Z40) (Z39:40)
7 : (Z7) (Z8:7)	24 : (Z24) (Z25:24)	41 : (Z41) (Z42:41)
8 : (Z8) (Z9:8)	25 : (Z25) (Z26:25)	42 : (Z42) (Z43:42)
9 : (Z9) (Z10:9)	26 : (Z26) (Z27:26)	43 : (Z43) (Z44:43)
10 : (Z10) (Z20:10)	27 : (Z27) (Z28:27)	44 : (Z44) (Z45:44)
11 : (Z11) (Z21:11)	28 : (Z28) (Z29:28)	45 : (Z45) (Z46:45)
12 : (Z12) (Z11:12)	29 : (Z29) (Z30:29)	46 : (Z46) (Z47:46)
13 : (Z13) (Z12:13)	30 : (Z30) (Z40:30)	47 : (Z47) (Z48:47)
14 : (Z14) (Z13:14)	31 : (Z31) (Z41:31)	48 : (Z48) (Z49:48)
15 : (Z15) (Z14:15)	32 : (Z32) (Z31:32)	49 : (Z49) (Z50:49)
16 : (Z16) (Z15:16)	33 : (Z33) (Z32:33)	50 : (Z50)
17 : (Z17) (Z16:17)	34 : (Z34) (Z33:34)	

5.3. Parallel Topology

We have considered two types of parallel topologies as are shown in Figure 5.3



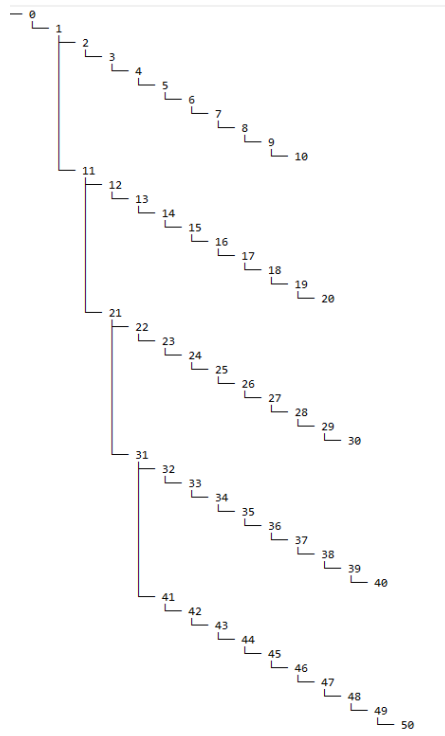
(a)



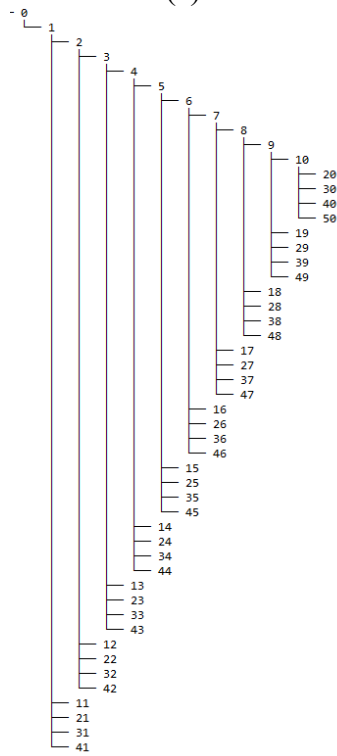
(b)

Figure 5.3. The considered parallel topologies (a) Type 1 (b) Type 2

The graph tree for these topologies are given in Figure 5.4.



(a)



(b)

Figure 5.4. The tree graph for the considered parallel topologies (a) Type 1 (b) Type 2

The impedance values for each node of the parallel topology type 1 are as follows

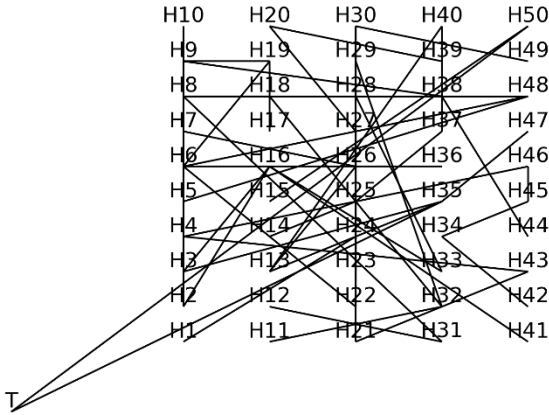
1 : (Z1) (Z2:1) (Z11:1)	18 : (Z18) (Z19:18)	35 : (Z35) (Z36:35)
2 : (Z2) (Z3:2)	19 : (Z19) (Z20:19)	36 : (Z36) (Z37:36)
3 : (Z3) (Z4:3)	20 : (Z20)	37 : (Z37) (Z38:37)
4 : (Z4) (Z5:4)	21 : (Z21) (Z22:21) (Z31:21)	38 : (Z38) (Z39:38)
5 : (Z5) (Z6:5)	22 : (Z22) (Z23:22)	39 : (Z39) (Z40:39)
6 : (Z6) (Z7:6)	23 : (Z23) (Z24:23)	40 : (Z40)
7 : (Z7) (Z8:7)	24 : (Z24) (Z25:24)	41 : (Z41) (Z42:41)
8 : (Z8) (Z9:8)	25 : (Z25) (Z26:25)	42 : (Z42) (Z43:42)
9 : (Z9) (Z10:9)	26 : (Z26) (Z27:26)	43 : (Z43) (Z44:43)
10 : (Z10)	27 : (Z27) (Z28:27)	44 : (Z44) (Z45:44)
11 : (Z11) (Z12:11) (Z21:11)	28 : (Z28) (Z29:28)	45 : (Z45) (Z46:45)
12 : (Z12) (Z13:12)	29 : (Z29) (Z30:29)	46 : (Z46) (Z47:46)
13 : (Z13) (Z14:13)	30 : (Z30)	47 : (Z47) (Z48:47)
14 : (Z14) (Z15:14)	31 : (Z31) (Z32:31) (Z41:31)	48 : (Z48) (Z49:48)
15 : (Z15) (Z16:15)	32 : (Z32) (Z33:32)	49 : (Z49) (Z50:49)
16 : (Z16) (Z17:16)	33 : (Z33) (Z34:33)	50 : (Z50)
17 : (Z17) (Z18:17)	34 : (Z34) (Z35:34)	

and for the parallel topology of type 2 are equal to

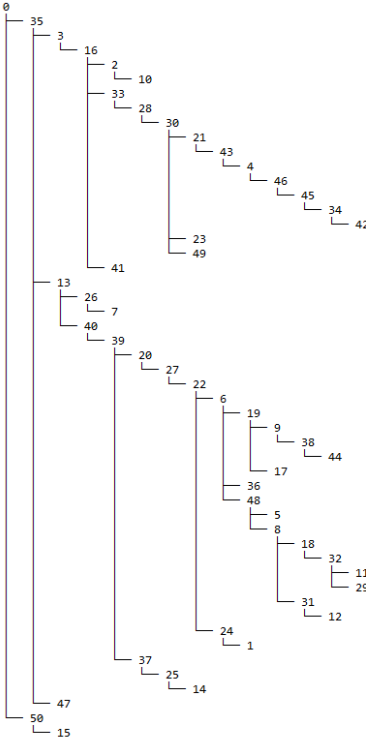
1 : (Z1) (Z2:1) (Z11:1) (Z21:1) (Z31:1) (Z41:1)		
2 : (Z2) (Z3:2) (Z12:2) (Z22:2) (Z32:2) (Z42:2)		
3 : (Z3) (Z4:3) (Z13:3) (Z23:3) (Z33:3) (Z43:3)		
4 : (Z4) (Z5:4) (Z14:4) (Z24:4) (Z34:4) (Z44:4)		
5 : (Z5) (Z6:5) (Z15:5) (Z25:5) (Z35:5) (Z45:5)		
6 : (Z6) (Z7:6) (Z16:6) (Z26:6) (Z36:6) (Z46:6)		
7 : (Z7) (Z8:7) (Z17:7) (Z27:7) (Z37:7) (Z47:7)		
8 : (Z8) (Z9:8) (Z18:8) (Z28:8) (Z38:8) (Z48:8)		
9 : (Z9) (Z10:9) (Z19:9) (Z29:9) (Z39:9) (Z49:9)		
10 : (Z10) (Z20:10) (Z30:10) (Z40:10) (Z50:10)		
11 : (Z11)	28 : (Z28)	45 : (Z45)
12 : (Z12)	29 : (Z29)	46 : (Z46)
13 : (Z13)	30 : (Z30)	47 : (Z47)
14 : (Z14)	31 : (Z31)	48 : (Z48)
15 : (Z15)	32 : (Z32)	49 : (Z49)
16 : (Z16)	33 : (Z33)	50 : (Z50)
17 : (Z17)	34 : (Z34)	
18 : (Z18)	35 : (Z35)	
19 : (Z19)	36 : (Z36)	
20 : (Z20)	37 : (Z37)	
21 : (Z21)	38 : (Z38)	
22 : (Z22)	39 : (Z39)	
23 : (Z23)	40 : (Z40)	
24 : (Z24)	41 : (Z41)	
25 : (Z25)	42 : (Z42)	
26 : (Z26)	43 : (Z43)	
27 : (Z27)	44 : (Z44)	

5.4. Random Topology

Finally, a random topology using the method given in the previous chapter has been constructed, as is given in Figure 5.5.



(a)



(b)

Figure 5.5. (a) A random topology layout and (b) its graph tree

The impedance values for each node of this topology are as follows

1 : (Z1)	26 : (Z26) (Z7:26)
2 : (Z2) (Z10:2)	27 : (Z27) (Z22:27)
3 : (Z3) (Z16:3)	28 : (Z28) (Z30:28)
4 : (Z4) (Z46:4)	29 : (Z29)
5 : (Z5)	30 : (Z30) (Z21:30) (Z23:30) (Z49:30)
6 : (Z6) (Z19:6) (Z36:6) (Z48:6)	31 : (Z31) (Z12:31)
7 : (Z7)	32 : (Z32) (Z11:32) (Z29:32)
8 : (Z8) (Z18:8) (Z31:8)	33 : (Z33) (Z28:33)
9 : (Z9) (Z38:9)	34 : (Z34) (Z42:34)
10 : (Z10)	35 : (Z35) (Z3:35) (Z13:35) (Z47:35)
11 : (Z11)	36 : (Z36)
12 : (Z12)	37 : (Z37) (Z25:37)
13 : (Z13) (Z26:13) (Z40:13)	38 : (Z38) (Z44:38)
14 : (Z14)	39 : (Z39) (Z20:39) (Z37:39)
15 : (Z15)	40 : (Z40) (Z39:40)
16 : (Z16) (Z2:16) (Z33:16) (Z41:16)	41 : (Z41)
17 : (Z17)	42 : (Z42)
18 : (Z18) (Z32:18)	43 : (Z43) (Z4:43)
19 : (Z19) (Z9:19) (Z17:19)	44 : (Z44)
20 : (Z20) (Z27:20)	45 : (Z45) (Z34:45)
21 : (Z21) (Z43:21)	46 : (Z46) (Z45:46)
22 : (Z22) (Z6:22) (Z24:22)	47 : (Z47)
23 : (Z23)	48 : (Z48) (Z5:48) (Z8:48)
24 : (Z24) (Z1:24)	49 : (Z49)
25 : (Z25) (Z14:25)	50 : (Z50) (Z15:50)

5.5. Performance Comparison

By using the impedance value at each node and the methods provided in the previous chapter, we calculated the transfer function between DC and every meter in each topology. The average value of the transfer function between all nodes and DC is provided in Figure 5.6. The plot is given over the CENELEC band frequency range. As it can be seen, the performance is achieved by the sequential topology followed by the parallel type 2. The reason can be as a result of higher reflection over branches with a longer length. The branches in the sequential topology are only a few meters long to connect the backbone LV lines to each meter. By comparing the two parallel topologies, it can be observed that the performance of the one that has shorter branches is better. Therefore, having longer branches in the LV network has a negative effect on the performance of the AMI system. This can also be studied based on the height of a graph for each topology, like the ones that have shorter trees on average a better performance.

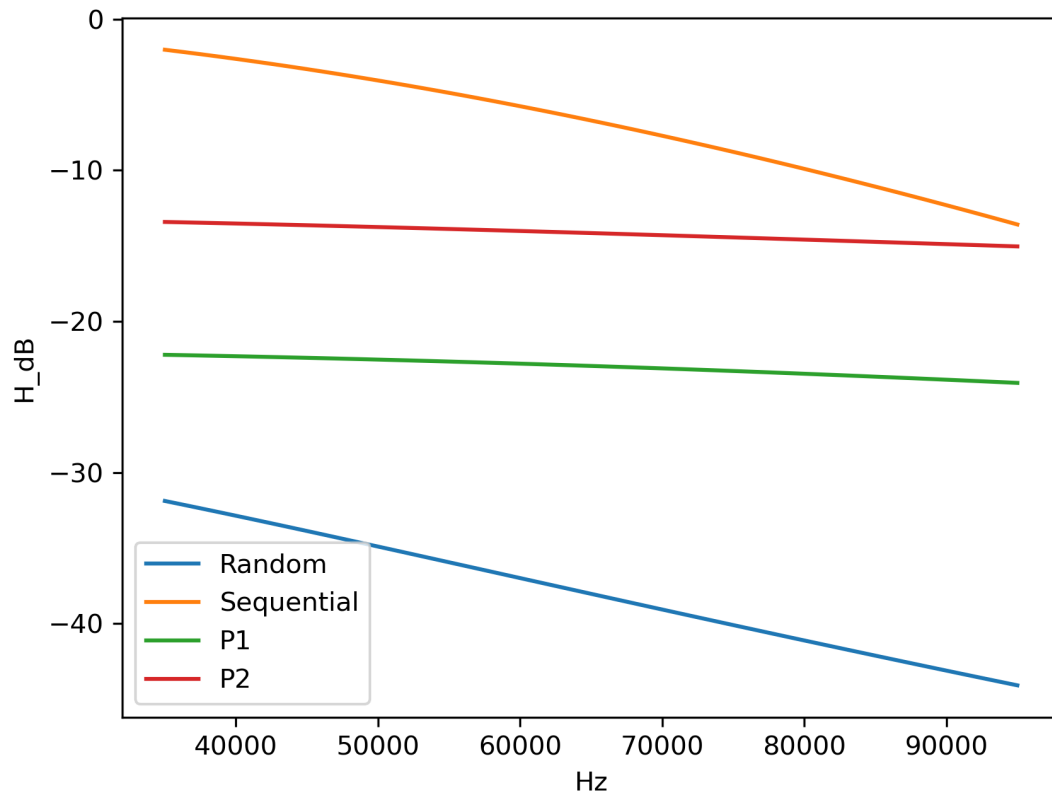


Figure 5.6. The average magnitude of transfer function for different topologies for CENELEC-A band

5.6. Summary

In this chapter, different topologies have been considered to study their effects on the performance of an AMI network. To calculate the transfer function, first, the impedance value at each node has been obtained. Using the PLC channel modelling discussed in Chapter 4, the transfer function between every meter and the DC in each topology has been calculated. Then the average value of the transfer function's magnitude for different topologies has been compared. It was shown that having longer branches in the LV network has a negative effect on the performance of the AMI system.

Chapter 6 : CONCLUSION AND RECOMMENDATION

6.1. Conclusion

Constant monitoring and control of the grid are the essential parts of the SG operation. To achieve this, having a widespread sensor network for monitoring the grid's status and an effective communication infrastructure for transferring the collected information and control signals across the grid is required. The smart metering system, also known as AMI, is a major part of the SG's monitoring and communication network, and its establishment is considered as an early step in the realization of the SG. The AMI employs information and communication technology for providing bi-directional communication links between SMs on the prosumer's side and the UC's data and control centres.

Currently, the considered applications of the AMI in South Africa are the remote recording of power consumption, implementation of TOU tariff and load limiting. Although such applications are not much sensitive to data-transmission latencies and communication outages, employing the AMI for more advanced SG applications, such as load management and controlling distributed generation and storage units, requires further considerations. To effectively support SG applications, an AMI network has to meet a specific level of interoperability, scalability, security and QoS depending on the considered SG application. The QoS demonstrates the reliability of communication links and their performance in the sense of data-rate and latency.

In Chapter 2, first, an overview of the AMI system was provided, and the communication requirements for different applications were discussed. As it was mentioned, the AMI communication network is divided into three sub-networks: HAN, which links SMs to in-home smart appliances; NAN, which covers communications between SMs and DCs; and WAN, which consists of communication links between DCs and MDMS. Since the focus of this research was on the NAN part of the network, the wireless and wireline technologies and standards used at different layers of AMI networks, with an emphasis on the AMI NAN standards, were discussed. This included the NB-PLC as the most widely used technology for AMI NAN in urban areas. Finally, a literature review has been provided on the studies that have been made on modelling, analysing and improving the performance of the two most used NB-PLC standards: PRIME and G3-PLC.

Chapter 3 provided an overview of the smart metering standard in South Africa. For this purpose, the specifications of the DLMS/COSEM and G3-PLC standard have been discussed. DLMS/COSEM is a suite of standards covering data exchange and interface modelling of metering devices, and it can be implemented on top of different lower layer standards and technologies. The communication model of G3-PLC consists of the UDP/IP6 layer, RFC 4944 adaption layer, IEEE 802.15.4 MAC layer and an OFDM-based physical layer. We discussed the data exchange between SMs and DC. We also covered the format of data sequence at each layer of the G3-PLC standard in order to provide a clear picture of the G3-PLC and its functionality.

To investigate a PLC-based AMI system thoroughly, one needs to have access to the power grid infrastructure. However, studying the effects of network parameters and topology on an actual AMI network can become very expensive. Simulation tools, on the other hand, are feasible approaches that can provide an insight into the effect of topology on the performance of a PLC-based AMI network. Therefore, in Chapter 4, the mathematical model of the system used to study the topology effect on the performance of the G3-PLC AMI network was derived. We began by modelling the consumption load to identify a realistic model for the number of meters connected to a DC and the type of suitable cable for being used in the model. This followed by proposing the bottom-up approach to calculate the transfer function between any two nodes in the network. We discussed the suitability of this method to study the effect of topology on the performance of the AMI system. We then derived the noise model and the capacity of the channel in accordance with the G3-PLC standard and proposed an indicator factor to compare the performance of different topologies. Further discussions have been made on modelling and simulating realistic topologies for the AMI network. Also, an algorithm has been proposed to calculate the transfer function between different nodes in the network.

By using the models and algorithms derived in Chapter 4, different topologies for the AMI network have been considered in Chapter 5, and their performance has been compared. It was shown that having longer branches in the LV network has a negative effect on the performance of the AMI system. This can be a starting point to consider the AMI performance in designing an LV distribution network.

6.2. Recommendation

This study has shown that the AMI network's topology has an effect on the performance of the system. However, designing the optimal topology for a distribution network requires further studies. For instance, there are many electrical and geographical constraints that limit the choice of a selected topology. As a recommendation for a future study, the optimization of a distribution network by thoroughly considering the electrical system's constraint can be studied where the requirement is to maximize the capacity of the AMI network.

REFERENCES

- [1] C.-H. Lo and N. Ansari, "The Progressive Smart Grid System from Both Power and Communications Aspects," *IEEE Communications Surveys & Tutorials*, vol. 14, no. 3, pp. 799-821, 2011.
- [2] M. Kolhe, "Smart Grid: Charting a New Energy Future: Research, Development and Demonstration," *The Electricity Journal*, vol. 25, no. 2, pp. 88-93, 2012.
- [3] M. H. Rehmani, M. Reisslein, A. Rachedi, M. Erol-Kantarci, and M. Radenkovic, "Integrating Renewable Energy Resources into the Smart Grid: Recent Developments in Information and Communication Technologies," *IEEE Transactions on Industrial Informatics*, vol. 14, no. 7, pp. 2814-2825, 2018.
- [4] I. Colak, S. Sagiroglu, G. Fulli, M. Yesilbudak, and C.-F. Covrig, "A Survey on the Critical Issues in Smart Grid Technologies," *Renewable and Sustainable Energy Reviews*, vol. 54, pp. 396-405, 2016.
- [5] "Smart Grid Market by Software (Ami, Grid Distribution, Grid Network, Grid Asset, Grid Security, Substation Automation, and Billing & Cis), Hardware (Smart Meter), Service (Consulting, Integration, and Support), and Region." <https://www.marketsandmarkets.com/Market-Reports/smart-grid-market-208777577.html> (accessed 2020).
- [6] H. Khurana, M. Hadley, N. Lu, and D. A. Frincke, "Smart-Grid Security Issues," *IEEE Security & Privacy*, vol. 8, no. 1, pp. 81-85, 2010.
- [7] J. Wu, S. Guo, H. Huang, W. Liu, and Y. Xiang, "Information and Communications Technologies for Sustainable Development Goals: State-of-the-Art, Needs and Perspectives," *IEEE Communications Surveys & Tutorials*, vol. 20, no. 3, pp. 2389-2406, 2018.
- [8] N. Uribe-Pérez, L. Hernández, D. De La Vega, and I. Angulo, "State of the Art and Trends Review of Smart Metering in Electricity Grids," *Applied Sciences*, vol. 6, no. 3, p. 68, 2016.
- [9] Y. Wang, Q. Chen, T. Hong, and C. Kang, "Review of Smart Meter Data Analytics: Applications, Methodologies, and Challenges," *IEEE Transactions on Smart Grid*, vol. 10, no. 3, pp. 3125-3148, 2018.
- [10] J. Wu, S. Guo, J. Li, and D. Zeng, "Big Data Meet Green Challenges: Greening Big Data," *IEEE Systems Journal*, vol. 10, no. 3, pp. 873-887, 2016.
- [11] J. Wu, S. Guo, J. Li, and D. Zeng, "Big Data Meet Green Challenges: Big Data toward Green Applications," *IEEE Systems Journal*, vol. 10, no. 3, pp. 888-900, 2016.
- [12] Y. Yan, Y. Qian, H. Sharif, and D. Tipper, "A Survey on Smart Grid Communication Infrastructures: Motivations, Requirements and Challenges," *IEEE communications surveys & tutorials*, vol. 15, no. 1, pp. 5-20, 2012.
- [13] S. Erlinghagen, B. Lichtensteiger, and J. Markard, "Smart Meter Communication Standards in Europe—a Comparison," *Renewable and Sustainable Energy Reviews*, vol. 43, pp. 1249-1262, 2015.
- [14] R. Deblasio and C. Tom, "Standards for the Smart Grid," in *2008 IEEE Energy 2030 Conference*, 2008: IEEE, pp. 1-7.
- [15] H. Groenewald, "Nrs049-Advanced Metering Infrastructure (Ami) for Residential and Commercial Customers," *ESKOM, Johannesburg, Presentation*, 2009.
- [16] X. Fang, S. Misra, G. Xue, and D. Yang, "Smart Grid—the New and Improved Power Grid: A Survey," *IEEE communications surveys & tutorials*, vol. 14, no. 4, pp. 944-980, 2011.
- [17] J. Bryson and P. Gallagher, "Nist Framework and Roadmap for Smart Grid Interoperability Standards, Release 2.0," *National Institute of Standards and Technology (NIST), Tech. Rep. NIST Special Publication 1108R2*, pp. 2-0, 2012.
- [18] C. Muscas, M. Pau, P. A. Pegoraro, and S. Sulis, "Smart Electric Energy Measurements in Power Distribution Grids," *IEEE Instrumentation & Measurement Magazine*, vol. 18, no. 1, pp. 17-21, 2015.

- [19] F. Li *et al.*, "Smart Transmission Grid: Vision and Framework," *IEEE transactions on Smart Grid*, vol. 1, no. 2, pp. 168-177, 2010.
- [20] Z. Fan *et al.*, "Smart Grid Communications: Overview of Research Challenges, Solutions, and Standardization Activities," *IEEE Communications Surveys & Tutorials*, vol. 15, no. 1, pp. 21-38, 2012.
- [21] S. E. Collier, "Ten Steps to a Smarter Grid," *IEEE Industry Applications Magazine*, vol. 16, no. 2, pp. 62-68, 2010.
- [22] H. Farhangi, "The Path of the Smart Grid," *IEEE power and energy magazine*, vol. 8, no. 1, pp. 18-28, 2009.
- [23] T. Hargreaves, M. Nye, and J. Burgess, "Making Energy Visible: A Qualitative Field Study of How Householders Interact with Feedback from Smart Energy Monitors," *Energy policy*, vol. 38, no. 10, pp. 6111-6119, 2010.
- [24] S. Darby, "The Effectiveness of Feedback on Energy Consumption," *A Review for DEFRA of the Literature on Metering, Billing and direct Displays*, vol. 486, no. 2006, p. 26, 2006.
- [25] T. Khalifa, K. Naik, and A. Nayak, "A Survey of Communication Protocols for Automatic Meter Reading Applications," *IEEE Communications Surveys & Tutorials*, vol. 13, no. 2, pp. 168-182, 2010.
- [26] Y. Kabalci, "A Survey on Smart Metering and Smart Grid Communication," *Renewable and Sustainable Energy Reviews*, vol. 57, pp. 302-318, 2016.
- [27] X. Fan and G. Gong, "Security Challenges in Smart-Grid Metering and Control Systems," *Technology Innovation Management Review*, vol. 3, no. 7, 2013.
- [28] J. Zhou, R. Q. Hu, and Y. Qian, "Scalable Distributed Communication Architectures to Support Advanced Metering Infrastructure in Smart Grid," *IEEE Transactions on Parallel and Distributed Systems*, vol. 23, no. 9, pp. 1632-1642, 2012.
- [29] V. C. Gungor *et al.*, "A Survey on Smart Grid Potential Applications and Communication Requirements," *IEEE Transactions on industrial informatics*, vol. 9, no. 1, pp. 28-42, 2012.
- [30] K. Sharma and L. M. Saini, "Performance Analysis of Smart Metering for Smart Grid: An Overview," *Renewable and Sustainable Energy Reviews*, vol. 49, pp. 720-735, 2015.
- [31] I. Sadinezhad and V. G. Agelidis, "Slow Sampling on-Line Harmonics/Interharmonics Estimation Technique for Smart Meters," *Electric Power Systems Research*, vol. 81, no. 8, pp. 1643-1653, 2011.
- [32] H. Li, R. Mao, L. Lai, and R. C. Qiu, "Compressed Meter Reading for Delay-Sensitive and Secure Load Report in Smart Grid," in *2010 First IEEE International Conference on Smart Grid Communications*, 2010: IEEE, pp. 114-119.
- [33] P. Siano, "Demand Response and Smart Grids—a Survey," *Renewable and sustainable energy reviews*, vol. 30, pp. 461-478, 2014.
- [34] H. S. Cho, T. Yamazaki, and M. Hahn, "Determining Location of Appliances from Multi-Hop Tree Structures of Power Strip Type Smart Meters," *IEEE Transactions on Consumer Electronics*, vol. 55, no. 4, pp. 2314-2322, 2009.
- [35] B. Bat-Erdene, B. Lee, M.-Y. Kim, T. H. Ahn, and D. Kim, "Extended Smart Meters-Based Remote Detection Method for Illegal Electricity Usage," *IET Generation, Transmission & Distribution*, vol. 7, no. 11, pp. 1332-1343, 2013.
- [36] R. R. Mohassel, A. Fung, F. Mohammadi, and K. Raahemifar, "A Survey on Advanced Metering Infrastructure," *International Journal of Electrical Power & Energy Systems*, vol. 63, pp. 473-484, 2014.
- [37] E. Ancillotti, R. Bruno, and M. Conti, "The Role of Communication Systems in Smart Grids: Architectures, Technical Solutions and Research Challenges," *Computer Communications*, vol. 36, no. 17-18, pp. 1665-1697, 2013.
- [38] V. C. Gungor and G. P. Hancke, "Industrial Wireless Sensor Networks: Challenges, Design Principles, and Technical Approaches," *IEEE Transactions on industrial electronics*, vol. 56, no. 10, pp. 4258-4265, 2009.
- [39] Q. Yang, J. A. Barria, and T. C. Green, "Communication Infrastructures for Distributed Control of Power Distribution Networks," *IEEE Transactions on Industrial Informatics*, vol. 7, no. 2, pp. 316-327, 2011.

- [40] R. H. Khan and J. Y. Khan, "A Comprehensive Review of the Application Characteristics and Traffic Requirements of a Smart Grid Communications Network," *Computer Networks*, vol. 57, no. 3, pp. 825-845, 2013.
- [41] E. Kabalci, Y. Kabalci, and I. Develi, "Modelling and Analysis of a Power Line Communication System with Qpsk Modem for Renewable Smart Grids," *International Journal of Electrical Power & Energy Systems*, vol. 34, no. 1, pp. 19-28, 2012.
- [42] P. Kumar, A. Braeken, A. Gurtov, J. Iinatti, and P. H. Ha, "Anonymous Secure Framework in Connected Smart Home Environments," *IEEE Transactions on Information Forensics and Security*, vol. 12, no. 4, pp. 968-979, 2017.
- [43] D. He, S. Chan, Y. Zhang, M. Guizani, C. Chen, and J. Bu, "An Enhanced Public Key Infrastructure to Secure Smart Grid Wireless Communication Networks," *IEEE Network*, vol. 28, no. 1, pp. 10-16, 2014.
- [44] M. Erol-Kantarci and H. T. Mouftah, "Energy-Efficient Information and Communication Infrastructures in the Smart Grid: A Survey on Interactions and Open Issues," *IEEE Communications Surveys & Tutorials*, vol. 17, no. 1, pp. 179-197, 2014.
- [45] V. C. Gungor *et al.*, "Smart Grid Technologies: Communication Technologies and Standards," *IEEE transactions on Industrial informatics*, vol. 7, no. 4, pp. 529-539, 2011.
- [46] R. Mao and V. Julka, "Wimax for Advanced Metering Infrastructure," in *2012 International Conference on Green and Ubiquitous Technology, 2012: IEEE*, pp. 15-19.
- [47] E. Yaacoub and A. Abu-Dayya, "Automatic Meter Reading in the Smart Grid Using Contention Based Random Access over the Free Cellular Spectrum," *Computer Networks*, vol. 59, pp. 171-183, 2014.
- [48] V. C. Gungor *et al.*, "Smart Grid and Smart Homes: Key Players and Pilot Projects," *IEEE Industrial Electronics Magazine*, vol. 6, no. 4, pp. 18-34, 2012.
- [49] S. Jain, "Pragmatic Agency in Technology Standards Setting: The Case of Ethernet," *Research Policy*, vol. 41, no. 9, pp. 1643-1654, 2012.
- [50] I. E. Commission, "Electricity Metering—Data Exchange for Meter Reading, Tariff and Load Control," *IEC-62056 Parts*, vol. 21, pp. 31-51, 2002.
- [51] Dlms User Association. www.dlms.com, (accessed 2020).
- [52] S. Feuerhahn, M. Zillgith, C. Wittwer, and C. Wietfeld, "Comparison of the Communication Protocols Dlms/Cosem, Sml and Iec 61850 for Smart Metering Applications," in *2011 IEEE International Conference on Smart Grid Communications (SmartGridComm)*, 2011: IEEE, pp. 410-415.
- [53] G. Wu, S. Talwar, K. Johnsson, N. Himayat, and K. D. Johnson, "M2m: From Mobile to Embedded Internet," *IEEE Communications Magazine*, vol. 49, no. 4, pp. 36-43, 2011.
- [54] N. Kushalnagar, G. Montenegro, and C. Schumacher, "Ipv6 over Low-Power Wireless Personal Area Networks (6lowpans): Overview, Assumptions, Problem Statement, and Goals," 2007.
- [55] M. Dohler, D. Barthel, T. Watteyne, and T. Winter, "Routing Requirements for Urban Low-Power and Lossy Networks," 2009.
- [56] P. Kulkarni, S. Gormus, Z. Fan, and B. Motz, "A Self-Organising Mesh Networking Solution Based on Enhanced Rpl for Smart Metering Communications," in *2011 IEEE International Symposium on a World of Wireless, Mobile and Multimedia Networks*, 2011: IEEE, pp. 1-6.
- [57] T. Watteyne, A. Molinaro, M. G. Richichi, and M. Dohler, "From Manet to Ietf Roll Standardization: A Paradigm Shift in Wsn Routing Protocols," *IEEE Communications Surveys & Tutorials*, vol. 13, no. 4, pp. 688-707, 2010.
- [58] A. A. Atayero, A. Alatishe, and Y. A. Ivanov, "Power Line Communication Technologies: Modeling and Simulation of Prime Physical Layer," in *World Congress on Engineering and Computer Science*, 2012, vol. 2, pp. 931-936.
- [59] M. Biagi, S. Greco, and L. Lampe, "Geo-Routing Algorithms and Protocols for Power Line Communications in Smart Grids," *IEEE Transactions on Smart Grid*, vol. 9, no. 2, pp. 1472-1481, 2016.

- [60] F. Aalamifar and L. Lampe, "Optimized Data Acquisition Point Placement for an Advanced Metering Infrastructure Based on Power Line Communication Technology," *IEEE Access*, vol. 6, pp. 45347-45358, 2018.
- [61] A. F. Olivera, A. S. Escalona, I. U. Galdos, J. M. Arenas, P. A. Buceta, and J. F. Vázquez, "Analysis of Prime Plc Smart Metering Networks Performance," in *Proc. Int. Conf. Renew. Energies Power Quality (ICREPO)*, 2013, p. 6.
- [62] A. Sendin, I. Berganza, A. Arzuaga, A. Pulkkinen, and I. H. Kim, "Performance Results from 100,000+ Prime Smart Meters Deployment in Spain," in *2012 IEEE Third International Conference on Smart Grid Communications (SmartGridComm)*, 2012: IEEE, pp. 145-150.
- [63] K. Razazian, A. Kamalizad, M. Umari, Q. Qu, V. Loginov, and M. Navid, "G3-Plc Field Trials in Us Distribution Grid: Initial Results and Requirements," in *2011 IEEE International Symposium on Power Line Communications and Its Applications*, 2011: IEEE, pp. 153-158.
- [64] K. Razazian, A. Niktash, V. Loginov, J. Leclare, T. Lys, and C. Lavenu, "Experimental and Field Trial Results of Enhanced Routing Based on Load for G3-Plc," in *2013 IEEE 17th International Symposium on Power Line Communications and Its Applications*, 2013: IEEE, pp. 149-154.
- [65] M. Korki, C. Zhang, and H. L. Vu, "Performance Evaluation of Prime in Smart Grid," in *2013 IEEE International Conference on Smart Grid Communications (SmartGridComm)*, 2013: IEEE, pp. 294-299.
- [66] I. H. Kim, B. Varadarajan, and A. Dabak, "Performance Analysis and Enhancements of Narrowband Ofdm Powerline Communication Systems," in *2010 First IEEE International Conference on Smart Grid Communications*, 2010: IEEE, pp. 362-367.
- [67] J. Matanza, S. Alexandres, and C. Rodríguez-Morcillo, "Advanced Metering Infrastructure Performance Using European Low-Voltage Power Line Communication Networks," *Iet Communications*, vol. 8, no. 7, pp. 1041-1047, 2014.
- [68] L. González-Sotres, C. Mateo, P. Frías, C. Rodríguez-Morcillo, and J. Matanza, "Replicability Analysis of Plc Prime Networks for Smart Metering Applications," *IEEE Transactions on Smart Grid*, vol. 9, no. 2, pp. 827-835, 2016.
- [69] L. Di Bert, S. D'alessandro, and A. M. Tonello, "A G3-Plc Simulator for Access Networks," in *18th IEEE International Symposium on Power Line Communications and Its Applications*, 2014: IEEE, pp. 99-104.
- [70] "Simprime: Simprime Official Site " <https://www.iit.comillas.edu/oferta-tecnologica/simprime> (accessed 2020).
- [71] M. Seijo, G. López, J. Matanza, and J. I. Moreno, "From the Lap (Top) to the Jungle: Validating the Prime Network Simulator Simprime with Data from the Field," in *2019 IEEE International Symposium on Power Line Communications and its Applications (ISPLC)*, 2019: IEEE, pp. 1-6.
- [72] K. Razazian, M. Umari, and A. Kamalizad, "Error Correction Mechanism in the New G3-Plc Specification for Powerline Communication," in *ISPLC2010*, 2010: IEEE, pp. 50-55.
- [73] A. Mengi and A. H. Vinck, "Successive Impulsive Noise Suppression in Ofdm," in *ISPLC2010*, 2010: IEEE, pp. 33-37.
- [74] T. Banwell and S. Galli, "A New Approach to the Modeling of the Transfer Function of the Power Line Channel," in *Proceedings of the 5th International Symposium on Power-Line Communications and its Applications (ISPLC)*, 2001: Citeseer, pp. 4-6.
- [75] L. González-Sotres, P. Frías, and C. Mateo, "Power Line Communication Transfer Function Computation in Real Network Configurations for Performance Analysis Applications," *Iet Communications*, vol. 11, no. 6, pp. 897-904, 2017.
- [76] O. G. Hooijen, "A Channel Model for the Residential Power Circuit Used as a Digital Communications Medium," *IEEE transactions on electromagnetic compatibility*, vol. 40, no. 4, pp. 331-336, 1998.
- [77] M. Nassar, J. Lin, Y. Mortazavi, A. Dabak, I. H. Kim, and B. L. Evans, "Local Utility Power Line Communications in the 3–500 Khz Band: Channel Impairments, Noise, and Standards," *IEEE signal processing magazine*, vol. 29, no. 5, pp. 116-127, 2012.

- [78] A. Sanz, D. Sancho, C. Guemes, and J. A. Cortés, "A Physical Layer Model for G3-Plc Networks Simulation," in *2017 IEEE International Symposium on Power Line Communications and its Applications (ISPLC)*, 2017: IEEE, pp. 1-6.
- [79] L. C. Garcia, A. E. Dulay, and G. M. I. Oseña, "Weighted-Probability Random Number Generator for Plc Channel Transfer Function Generation," *Engineering Journal*, vol. 24, no. 1, pp. 185-197, 2020.
- [80] M. Korki, H. L. Vu, C. H. Foh, X. Lu, and N. Hosseinzadeh, "Mac Performance Evaluation in Low Voltage Plc Networks," *ENERGY*, vol. 135, 2011.
- [81] G. Patti, G. Alderisi, and L. L. Bello, "Performance Assessment of the Prime Mac Layer Protocol," in *2013 11th IEEE International Conference on Industrial Informatics (INDIN)*, 2013: IEEE, pp. 158-164.
- [82] Q. Weiqiang, C. Bingbing, and W. Xianpei, "Research on Dynamic Trust Evaluation Mechanism of Mac Layer in G3-Plc," in *2020 IEEE International Conference on Artificial Intelligence and Information Systems (ICAIS)*, 2020: IEEE, pp. 753-756.
- [83] A. Ikpehai and B. Adebisi, "6loplc for Smart Grid Applications," in *2015 IEEE International Symposium on Power Line Communications and Its Applications (ISPLC)*, 2015: IEEE, pp. 211-215.
- [84] H. C. Ferreira, L. Lampe, J. Newbury, and T. G. Swart, *Power Line Communications: Theory and Applications for Narrowband and Broadband Communications over Power Lines*. John Wiley & Sons, 2011.
- [85] G. Bumiller, *Single Frequency Network Technology for Fast Ad Hoc Communication Networks over Power Lines*. WiKu-Wiss.-Verlag Stein, 2009.
- [86] G. Bumiller, L. Lampe, and H. Hrasnica, "Power Line Communication Networks for Large-Scale Control and Automation Systems," *IEEE Communications Magazine*, vol. 48, no. 4, pp. 106-113, 2010.
- [87] M. Biagi and L. Lampe, "Location Assisted Routing Techniques for Power Line Communication in Smart Grids," in *2010 First IEEE International Conference on Smart Grid Communications*, 2010: IEEE, pp. 274-278.
- [88] N. Bressan, L. Bazzaco, N. Bui, P. Casari, L. Vangelista, and M. Zorzi, "The Deployment of a Smart Monitoring System Using Wireless Sensor and Actuator Networks," in *Smart Grid Communications (SmartGridComm), 2010 First IEEE International Conference on*, 2010, pp. 49-54.
- [89] S. Dawson-Haggerty, A. Tavakoli, and D. Culler, "Hydro: A Hybrid Routing Protocol for Low-Power and Lossy Networks," in *Proc. IEEE Int. Conf. Smart Grid Commun. (SmartGridComm)*, 2010, pp. 268-273.
- [90] F. Marcuzzi and A. M. Tonello, "Artificial-Intelligence-Based Performance Enhancement of the G3-Plc Loadng Routing Protocol for Sensor Networks," in *2019 IEEE International Symposium on Power Line Communications and its Applications (ISPLC)*, 2019: IEEE, pp. 1-6.
- [91] Y. Cui, X. Liu, J. Cao, and D. Xu, "Network Performance Optimization for Low-Voltage Power Line Communications," *Energies*, vol. 11, no. 5, p. 1266, 2018.
- [92] R. Atat, M. Ismail, M. F. Shaaban, E. Serpedin, and T. Overbye, "Stochastic Geometry-Based Model for Dynamic Allocation of Metering Equipment in Spatio-Temporal Expanding Power Grids," *IEEE Transactions on Smart Grid*, vol. 11, no. 3, pp. 2080-2091, 2019.
- [93] S. Panchadcharam, G. Taylor, Q. Ni, I. Pisica, and S. Fateri, "Performance Evaluation of Smart Metering Infrastructure Using Simulation Tool," in *2012 47th International Universities Power Engineering Conference (UPEC)*, 2012: IEEE, pp. 1-6.
- [94] A. Gogic, A. Mahmutbegovic, D. Borovina, İ. H. Çavdar, and N. Suljanovic, "Simulation of the Narrow-Band Plc System Implementing Prime Standard," in *2014 IEEE International Energy Conference (ENERGYCON)*, 2014: IEEE, pp. 1520-1525.
- [95] J. Larrañaga, J. Legarda, I. Urrutia, and A. Sendin, "An Experimentally Validated Prime Subnetwork Simulation Model for Utility Applications," in *2015 IEEE International Symposium on Power Line Communications and Its Applications (ISPLC)*, 2015: IEEE, pp. 95-100.
- [96] S. G. S. Group, "Iec Smart Grid Standardization Roadmap," 2010, vol. Ed 1.0.
- [97] Nrs. "National Regulatory Services." www.nrs.eskom.co.za (accessed 2021).

- [98] J. Anatory, N. Theethayi, R. Thottappillil, M. Kissaka, and N. H. Mvungi, "The Influence of Load Impedance, Line Length, and Branches on Underground Cable Power-Line Communications (Plc) Systems," *IEEE Transactions on Power Delivery*, vol. 23, no. 1, pp. 180-187, 2007.
- [99] *Iec 61000-2-2: Electromagnetic Compatibility (Emc)—Part 2-2: Environment—Compatibility Levels for Lowfrequency Conducted Disturbances and Signalling in Public Low-Voltage Power Supply Systems*, Iec, Geneva, Switzerland, 2018.
- [100] H. Philipps, "Performance Measurements of Powerline Channels at High Frequencies," in *Proceedings of the International Symposium on Power Line Communications and its Applications (ISPLC)*, 1998, vol. 229237.
- [101] B. Prahó, M. Tlich, P. Pagani, A. Zeddám, and F. Nouvel, "Cognitive Detection Method of Radio Frequencies on Power Line Networks," in *ISPLC2010*, 2010: IEEE, pp. 225-230.
- [102] M. Babic and K. Dostert, "An Fpga-Based High-Speed Emulation System for Powerline Channels," in *International Symposium on Power Line Communications and Its Applications, 2005.*, 2005: IEEE, pp. 290-294.
- [103] D. Middleton, "Statistical-Physical Models of Electromagnetic Interference," *IEEE transactions on Electromagnetic Compatibility*, no. 3, pp. 106-127, 1977.
- [104] R. Blum, Y. Zhang, B. Sadler, and R. Kozick, "On the Approximation of Correlated Non-Gaussian Noise Pdfs Using Gaussian Mixture Models," in *Conference on the Applications of Heavy Tailed Distributions in Economics, Engineering and Statistics*, 1999: Citeseer.
- [105] M. Zimmermann, "An Analysis of the Broadband Noise Scenario in Powerline Networks," in *Proc. 4th Int. Symp. Power Line Commun. Appl., Apr. 2000*, 2000, pp. 131-138.
- [106] H. Dai and H. V. Poor, "Advanced Signal Processing for Power Line Communications," *IEEE Communications Magazine*, vol. 41, no. 5, pp. 100-107, 2003.
- [107] T. Esmailian, F. R. Kschischang, and P. Glenn Gulak, "In-Building Power Lines as High-Speed Communication Channels: Channel Characterization and a Test Channel Ensemble," *International Journal of Communication Systems*, vol. 16, no. 5, pp. 381-400, 2003.
- [108] L. Di Bert, P. Caldera, D. Schwingshackl, and A. M. Tonello, "On Noise Modeling for Power Line Communications," in *2011 IEEE International Symposium on Power Line Communications and Its Applications*, 2011: IEEE, pp. 283-288.
- [109] D. Liu, E. Flint, B. Gaucher, and Y. Kwark, "Wide Band Ac Power Line Characterization," *IEEE Transactions on Consumer Electronics*, vol. 45, no. 4, pp. 1087-1097, 1999.
- [110] *Series G: Transmission Systems and Media, Digital Systems and Networks*, Itu-T, 2017. [Online]. Available: <https://www.itu.int/rec/T-REC-G.9903/en>